

Title: Mutations in a *Golden2-like* gene cause reduced seed weight in barley *albino lemma 1* mutants.

Running title: Barley *albino lemma 1* mutant

Corresponding Author: Shin Taketa

Institute of Plant Science and Resources, Okayama University, 2-20-1 Chuo, Kurashiki 710-0046, Japan

Phone: +81-86-434-1237,

Fax: +81-86-434-1249

e-mail: staketa@rib.okayama-u.ac.jp

Subject areas: (1) growth and development, (5) photosynthesis, respiration and bioenergetics

Number of black and white figures, color figures, tables, and type and number of supplementary material:

4 black and white figures

4 color figures

1 table

4 supplementary figures

5 supplementary tables

Title:

Mutations in a *Golden2-like* gene cause reduced seed weight in barley *albino lemma 1* mutants

Running head:

Barley *albino lemma 1* mutant

Authors: Shin Taketa, Momoko Hattori, Tsuneaki Takami, Eiko Himi and Wataru Sakamoto

Authors' Addresses: Institute of Plant Science and Resources, Okayama University, 2-20-1 Chuo, Kurashiki 710-0046, Japan

Footnotes: The *HvGLK2* genomic sequence of cv. Morex reported in this paper has been submitted to the DDBJ database under accession number LC570959.

Abstract:

The *albino lemma 1* (*alm1*) mutants of barley (*Hordeum vulgare* L.) exhibit obvious chlorophyll-deficient hulls. Hulls are seed-enclosing tissues on the spike, consisting of the lemma and palea. The *alm1* phenotype is also expressed in the pericarp, culm nodes, and basal leaf sheaths, but leaf blades and awns are normal green. A single recessive nuclear gene controls tissue-specific *alm1* phenotypic expression. Positional cloning revealed that the *ALM1* gene encodes a Golden 2-like (GLK) transcription factor, *HvGLK2*, belonging to the GARP subfamily of Myb transcription factors. This conclusion was validated by genetic evidence indicating that all ten *alm1* mutants studied had a lesion in functionally important regions of *HvGLK2*, including the three alpha-helix domains, an AREAEAA motif, and the GCT box. Transmission electron microscopy revealed that, in lemmas of the *alm1.g* mutant, the chloroplasts lacked thylakoid membranes, instead of stacked thylakoid grana in wild-type chloroplasts. Compared with wild type, *alm1.g* plants were similar in leaf photosynthesis, but declined in spike photosynthesis by 34%. The *alm1.g* mutant and the *alm1.a* mutant declined in 100-grain weight by 15.8% and 23.1%, respectively. As in other plants, barley has *HvGLK2* and a paralog, *HvGLK1*. In flag leaves and awns, *HvGLK2* and *HvGLK1* are expressed at moderate levels, but in hulls, *HvGLK1* expression was barely detectable compared with *HvGLK2*. Barley *alm1/Hvglk2* mutants exhibit more severe phenotypes than *glk2* mutants of other plant species reported to date. The severe *alm1* phenotypic expression in multiple tissues indicates that *HvGLK2* has some roles that are non-redundant with *HvGLK1*.

Keywords: chloroplast, GLK2, *Hordeum vulgare*, photosynthesis, spike, thylakoid

Introduction

Barley (*Hordeum vulgare* L., $2n=2x=14$, genome H), the world's fourth most important cereal crop, belongs to the tribe Triticeae of the grass family Poaceae. With the benefits of a self-fertilizing diploid, earlier intensive mutation studies accumulated abundant mutants of artificial as well as spontaneous origin (Stadler, 1928, Gustafson et al. 1971, Lundqvist, 2014). Barley morphological mutants were used traditionally as visual markers for constructing a conventional linkage map that integrated about 200 loci (Lundqvist et al. 1997, Costa et al. 2001). Currently, these morphological mutants are receiving renewed attention for studying biological processes (Druka et al. 2011). Positional cloning of causal genes for barley mutants has become increasingly feasible, partly because ample DNA markers are readily available (Varshney et al. 2007, Sato et al. 2009). More importantly, the advanced DNA sequencing technologies generated high-quality barley genome sequences by overcoming its huge size (5.1 Gb) and complexity (> 80% repetitive sequences) (Mascher et al. 2017). Consequently, many genomics tools available for barley are facilitating the identification and functional characterization of various key morphological genes (e.g., Yoshikawa et al. 2016, Milner et al. 2019).

In barley, *albino lemma 1* (*alm1*, syn. *eburatum*) is a remarkable visible mutant. The *alm1* phenotype of whitish leaf sheath bases starts to manifest as early as during the seedling stage. The characteristic *alm1* phenotype of whitish spikes becomes apparent around the heading stage, but it recedes before the yellow ripening stage. The *alm1* phenotypes are expressed stably irrespective of environmental conditions such as temperature (Takahashi and Hayashi, 1959). The first *alm1* mutant, "Russia 82", which likely occurred spontaneously in an unknown cultivar, is assigned the allele symbol, *alm1.a*. The *alm1.a* mutant is controlled by a single nuclear recessive gene located on the short arm of barley chromosome 3H (Takahashi and Hayashi, 1959, Costa et al. 2001). To date, 11 *alm1* or *alm1*-like mutants have been catalogued (Franckowiack and Lundqvist, 2016). The causal gene for *alm1* remains unknown despite recent intensive molecular genetic approaches (Hua et al. 2016, Shmakov et al. 2016).

Another point of importance of the barley *alm1* mutant is its possible utility for photosynthesis (Nutbeam and Duffus, 1978, Watson and Duffus, 1988) and morphological research. The *alm1* mutants lack chlorophyll pigments in hulls, except for small green areas at the edge connecting to the awn, but they have normal green leaf blades and awns. Such unique properties of barley *alm1* mutants can allow non-destructive measurements of spike photosynthesis using a portable photosynthesis system. In an earlier study, spike photosynthesis was estimated by detachment, shading or ^{14}C -labelling experiments. These studies estimated that the photosynthetic contribution of the barley spikes (including awns) to grain yields of 13% – 38% (reviewed by Tambussi et al. 2007). No spike-specific albino mutants similar to barley *alm1* have been reported in other crops because white panicle

mutants in rice (*Oryza sativa*) and foxtail millet (*Setaria italica*) accompanied variegated leaves or weak growth (Song et al. 2014, Wang et al. 2016, Li et al. 2018, Sun et al. 2019).

With this study, we demonstrated using positional cloning that the barley *alm1* locus encodes a Golden 2-like (GLK) transcription factor: HvGLK2. This conclusion was verified based on results of analyses of ten allelic mutants with independent origin. GLK transcription factors are members of the GARP family of Myb transcription factors, as defined by Riechmann *et al.* (2000). Actually, GARP is an acronym of Golden2 in maize (*Zea mays*) (Jenkins, 1927, Hall et al. 1998), the *Arabidopsis thaliana* type B RESPONSE REGULATORS (ARR-B) proteins (Imamura et al. 1999) and the PHOSPHATE STARVATION RESPONSE1 (PSR1) protein of *Chlamydomonas reinhardtii* (Wykoff et al. 1999). Reportedly, GLK transcription factors play a crucially important role in chloroplast development in *Arabidopsis thaliana*, maize (*Zea mays*), rice, tomato (*Solanum lycopersicum*) and moss *Physcomitrella patens* (Rossini et al. 2001, Fitter et al. 2002, Yasumura et al. 2005, Waters et al. 2009, Nakamura et al. 2009, Kobayashi et al. 2012, Powell et al. 2012). Detailed analyses in *Arabidopsis thaliana* revealed that *GLK* genes induce nuclear genes related to light harvesting and chlorophyll biosynthesis (Waters et al. 2009). We describe the unique *alm1* phenotypes expressed in multiple tissues of barley with diverse genetic backgrounds. We also present expression patterns of the *HvGLK* genes and chloroplast anatomy that were studied in a near isogenic line pair of cv. Misato Golden (WT) and its *alm1.g* mutant (*alm-MG*). Furthermore, we examined the effects of the *alm1* gene on photosynthesis and agronomic characteristics using the same near isogenic line pair. Severe albino phenotypes expressed in multiple tissues of the barley *alm1* mutants suggest functional differentiation of *HvGLK2* from its paralog: *HvGLK1*.

Results

Positional cloning of *alm1*

Genetic mapping of the *alm1* locus was conducted in 157 F₂ plants derived from a cross between two linkage tester lines: KL15 (line carrying the *alm1.a* allele from Russia 82) and KL17 (normal green line). Public SSR and EST markers were used for initial mapping. The *alm1* locus was localized within a 3.2-cM interval flanked by markers k00904 and k07761, respectively, at the 1.0-cM distal and the 2.2-cM proximal side in the proximal region of the barley chromosome arm 3HS (**Supplementary Fig. S1**). Marker k00892 also colocalized with k07761, but k07761 is regarded as a closer flanking marker at the proximal side because k00892 located 0.9 cM apart from k07761 in a high-density genetic map by Sato *et al.* (2009).

To search for *alm1* candidate genes, we exploited micro-collinearity of our barley genetic map to the rice reference genome sequence of cv. Nipponbare. We consulted the MSU Rice Genome Annotation Project Database (<http://rice.plantbiology.msu.edu/>). We also used

the version of barley genome assembly Hv_IBSC_PGSB_v2 of cv. Morex (Masher et al. 2017), as viewed from the Ensembl Plants *Hordeum vulgare* database (http://plants.ensembl.org/Hordeum_vulgare/Info/Index). The barley *alm1* candidate region was estimated as having 62.5-Mb physical length. The gene order in this barley region is well conserved with a syntenic region of rice chromosome 1. The flanking barley markers, k00904 and k07761, corresponded to rice gene LOC_Os01g13280 and LOC_Os01g17430, respectively. The two rice genes were 2.82 Mb apart; 386 genes were annotated between them. Within the rice syntenic region, after we selected four genes that were apparently related to the *alm1* phenotype in rice gene annotations, we sought their barley orthologues. Then, polymorphisms between the barley mapping parents were sought by sequencing with specific primers. Polymorphic markers were developed (**Supplementary Table S1**). Two new CAPS markers, *HvClp1* (*putative chloroplast protease* gene) and *HvCRD1* (*copper response defect1* gene), were both mapped 1.9 cM proximally from *alm1*. This finding narrowed down the candidate region to a 2.9-cM interval in barley, which corresponded to 2.28 Mb in rice chromosome 1 and about 18 Mb in the barley 3H physical map (**Supplementary Fig. S1**). The other two markers, *HvWRKY1* (*WRKY1* gene) and *HvGLK2*, colocalized with *alm1*. It is noteworthy that *HvGLK2* of KL15 (*alm1.a* line) harbors an approximately 1-kb deletion relative to that of KL17 (normal line), which is predicted to lack critical regions of the gene. Available results implicate *HvGLK2* as a strong candidate gene underlying the *alm1* locus.

Validation of *alm1* cloning by sequencing ten mutant alleles

In the barley genome database, the *ALM1* candidate gene (*HvGLK2*) is assigned gene number HORVU3Hr1G032440 with annotation as a two-component response regulator-like ARABIDOPSIS PSEUDO RESPONSE REGULATOR2 (APRR2). However, its gene structure is incomplete because intron 1 has a gap of unknown size. The region surrounding this gap was recalcitrant to PCR amplification. We filled this intron 1 gap after substantial efforts. The intron 1 sequences of *HvGLK2* included poly-G stretches of 20–22 mer, which likely precluded PCR amplification. Results show that Morex, the cultivar selected for the barley genome sequencing project, has a stretch of 20 Gs within intron 1 of 973 nt long. Other barley accessions have a 20–22-mer poly-G stretch in intron 1. We decoded the complete genomic sequence of *HvGLK2* in ten *alm1* mutants and their original cultivars (**Supplementary Table S2**). The 20–22-mer poly-G stretch in intron 1 is apparently unique to the barley *HvGLK2* gene because our database searches revealed no similar stretch in the orthologues of six other plant species that we surveyed.

A comparison of the genomic sequence obtained in this study and a full length cDNA sequence in the database (EMBL/GenBank/DBJ accession number AK353571) revealed that the *HvGLK2* gene encompasses 4,905 bp with six exons and five introns and that its

coding sequence (CDS) encodes a deduced protein of 506 amino acids (aa) (**Fig. 1**). Amino acid sequences in *HvGLK2* were conserved among the four wild type cultivars that we studied (cvs. Morex, Foma, Misato Golden, and Nampu Hadaka), which represented major morphological diversity such as covered vs. naked caryopsis and two-rowed and six-rowed types. Genomic sequence variations of three kinds were detected within introns: (i) poly-G stretch number variation in intron 1 of 20–22, (ii) a C to T substitution in intron 2 of cv. Foma, and (iii) (AT)_n microsatellite repeat variation in intron 5 (eight or nine times) (**Supplementary Table S2**).

The *HvGLK2* genomic sequences of ten *alm1* mutants (one spontaneous and nine induced origin) were compared with those of their respective wild type. All ten *alm1* mutant lines had a lesion affecting the functionally important regions of *GLK2*, including the three alpha-helix domains, an AREAEAA motif, and the GCT box (**Fig. 1**). This finding validated our conclusion that *ALM1* is *HvGLK2*.

The present study classified ten *alm1* mutant lines into seven groups based on critical polymorphism causing aa changes (**Supplementary Table S2**). The original *alm1.a* mutant has a 969-bp deletion missing from exon 3 to exon 6. Nonsense mutation alleles of three types were found: *alm1.e* in Morex, *ebu-a.1* and *ebu-a.2* in Foma, and *alm1.g* in Misato Golden. Each mutant harbored a single nucleotide substitution that is predicted to stop translation at the 267th, 140th, and 387th aa positions. Three types of one or two bp-deletion alleles were found: *alm1.d* in Morex had a two-bp deletion in exon 3 (CA at 3867th nt); *ebu-a.3*, *ebu-a.4*, and *ebu-a.5* in Foma all had a one-bp deletion in exon 3 (G at 3818th nt); *alm1.h* in Nampu Hadaka had a one-bp deletion in exon 4 (C at 4243th nt). All these deletions are predicted to cause a frame shift that affects a functionally important motif or domain. The *alm1.g* mutant in Misato Golden and the *alm1.h* mutant in Nampu Hadaka, induced in Japan, are documented for the first time herein. The *ebu-a.1* and *ebu-a.2* mutants, which were isolated in Sweden, had an identical *HvGLK2* sequence. The remaining three mutants, *ebu-a.3*, *ebu-a.4*, and *ebu-a.5*, shared the same critical mutation in exon 3, but varied in terms of the poly-G stretch number of 20–22 mer within intron 1.

The *alm1.b*, *alm1.c*, and *alm1.f* mutants described in the barley gene catalog (Franckowiak and Lundqvist, 2016) were unavailable for this study. Franckowiak and Lundqvist (2016) assigned the *alm1.f* allele symbol to the *white husk* (*wh*) mutant of a Chinese malting barley cv. Supi 3, but this mutant was reported as showing small yellow spots on leaves (Hua et al. 2016), unlike the ten *alm1* mutants without leaf spots examined for the present study. Consequently, the *wh* mutant requires confirmation by an allelism test and gene sequencing.

Phenotypes of seven *alm1* allelic mutants

All seven types of *alm1* allelic mutants exhibit prominent white hulls that are devoid of chlorophyll pigments and seemed to be loss-of-function mutations (**Figs. 2, 3; Supplementary Fig. S2**). Hulls are seed-enclosing tissues of the spike, consisting of the lemma and palea. The *alm1* phenotype is also observed in multiple tissues such as the pericarp, node, and basal leaf sheath, but the main photosynthetic tissues such as culm internodes, leaf blades, and awns are normal green. Consequently, the *alm1* mutants can grow well and can produce viable seeds.

A barley spike has three one-flowered spikelets at each rachis node. The two lateral spikelets are small and sterile in two-rowed barley, but all three spikelets are developed and fertile in six-rowed barley. Central spikelets of *alm1* mutants exhibited albino hulls in both row types. In contrast, lateral spikelets in two-rowed *alm1* mutants had green hulls; those in six-rowed *alm1* mutants exhibited albino hulls (**Fig. 3; Supplementary Fig. S2**). Such a row-type-dependent *alm1* manifestation in lateral spikelets is unique to barley. Careful observations have shown that albino lemmas of the *alm1* mutants had a small green area at the edge connecting to awns. In addition, lateral spikelets of two-rowed *alm1* mutants were not entirely green: they had a whitish base. From such row-type dependent alteration of *alm1* manifestation, we speculate that organ size differences might be related to the appearance of *alm1* phenotype in lateral spikelets. The glumes, which are attached at the base to the lemma, were green both in WT and *alm1* mutants, irrespective of the row type.

Phylogenetic analyses of monocotyledonous and dicotyledonous GLK proteins

Plant-specific GLK2-like (GLK) transcription factor proteins generally exist in a pair: GLK1 and GLK2 (Chen et al. 2016). Barley genome database searching identified a paralog on the barley chromosome arm 7HL: *HvGLK1* (HORVU7Hr1G083690). The *HvGLK1* gene encodes a predicted protein of 459 aa. To assess the relation of GLK proteins in monocotyledonous and dicotyledonous species, phylogenetic analysis was conducted using the predicted GLK amino acid sequences of six plant species (barley, rice, maize, *Arabidopsis thaliana*, tomato, and pepper [*Capsicum annuum*]) collected through database searches. Multiple alignment showed that the AREAEAA motif just downstream of the third alpha-helix was conserved, except SlGLK1 and ZmGLK1, which existed as AREVEAA. The AARKW motif in exon 4 for GLK2 of rice and maize reported by Rossini *et al.* (2002) was also present in HvGLK2 (**Supplementary Fig. S3**). The Neighbor Joining phylogenetic tree (**Fig. 4**) showed that the GLK proteins examined in this study were divisible into clades of monocotyledonous and dicotyledonous species, and that each clade could be split further into subclades of GLK1 and GLK2, except for those from *Arabidopsis thaliana*. The close relation of AtGLK1 and AtGLK2 coincides with that described in an earlier report (Fitter et al. 2002). In

monocotyledonous GLK1 and GLK2 subclades, barley and rice occupied closer positions than maize, which branched basally from them.

Expression of *HvGLK2* and *HvGLK1* genes

Expression of *HvGLK2* and *HvGLK1* at the heading stage was studied using quantitative reverse transcription-PCR (qRT-PCR) in three tissues: flag leaves, awns, and hulls. The glyceraldehyde-3-phosphate dehydrogenase (*GAPDH*) gene was used as an internal normalizer. A near isogenic line pair of wild type cultivar “Misato Golden” (MG) and its *alm1.g* mutant (abbreviated as *alm1.g*-MG) were examined. This pair was selected because of their compact spikes (**Fig. 2**) and early flowering habit. The *alm1.g* mutant is a loss-of-function mutation having a premature stop codon at the 387th aa position. Expression levels of *HvGLK2* and *HvGLK1* in MG and *alm1.g*-MG were relatively high in flag leaves and intermediate in awns. In hulls, however, *HvGLK2* was weakly expressed in both lines, but *HvGLK1* expression was barely detectable in both lines (**Fig. 5**).

Agronomic characteristics

Agronomic characteristics were studied during three seasons using greenhouse-grown materials. In season 1 and 2, a near isogenic line pair of MG (WT) and *alm1.g*-MG mutant was examined. In season 3, an *alm1.g*-MG isogenic line derived from two times of backcrosses, described as *alm1.g*-MG (BC₂), was used. The results are presented in **Table 1**. Heading dates in *alm1.g*-MG were delayed by about four days relative to MG in all seasons. The culm length of *alm1.g*-MG (BC₂) was higher than that of MG in season 3. Spikes were longer in *alm1.g*-MG than in MG in seasons 1 and 3. Awn lengths and numbers of grains per spike were similar between *alm1.g* mutant and WT in all seasons. In all seasons, the 100-grain weight was significantly lower in *alm1.g*-MG than in MG. In fact, the reduction ranged 11.1% – 22.2% during the three seasons with the mean of 15.8%. Moreover, a near isogenic pair of Bowman and the *alm1.a* allele Bowman line were tested for grain weight during three seasons. The 100-grain weight of *alm1.a*- Bowman was significantly lighter than that of Bowman, with an average of 23.1% reduction (**Supplementary Table S3**). Consequently, observations on plural *alm1* mutant alleles in near isogenic line pairs indicated that the barley *alm1* mutations reduce grain weight.

Transmission electron microscopy

The ultrastructure of chloroplasts in lemmas 6 days after heading was examined using transmission electron microscopy (TEM) in a near isogenic line pair of MG (WT) and *alm1.g*-MG (**Fig. 6**). The MG chloroplasts had developed thylakoid membranes and stacked grana. Chloroplasts in *alm1.g*-MG were observed infrequently. They were almost half the size and were irregularly shaped. Moreover, *alm1.g*-chloroplasts had no thylakoid membranes. Some small vesicles were present internally. Consequently, TEM analysis indicated that the *alm1.g* mutation severely impaired chloroplast development in chlorophyll-deficient lemmas.

Chlorophyll content and photosynthesis ability in leaves and spikes

Chlorophyll contents of plants at 5 and 16 days after heading were estimated using a chlorophyll meter: Soil and Plant Analyzer Development (SPAD) (**Supplementary Table S4**). The SPAD values of flag leaves at 5 days after heading were significantly higher in *alm1.g*-MG than in MG. The SPAD values in MG were higher in the lemma than in the palea at both dates. Values increased as the days from heading proceeded. Along with TEM results, these observations indicated that thylakoid biogenesis in MG proceeds to allow photosynthetic carbon assimilation in the lemma and palea during spike development. In *alm1.g*-MG, however, SPAD values of the lemma and palea were below the detection limit at both dates, which agrees with results found by TEM observations for heavily impaired chloroplasts.

To measure photochemical efficiency, detached spikes at 16 days after heading were examined with a Pulse Amplitude Modulation (PAM) chlorophyll fluorescence detection system. The ratio of F_v/F_m represents the maximal photosynthetic efficiency of photosystem II (PSII), whereas non-photochemical quenching (NPQ) represents the ability to dissipate excess absorbed light energy non-photochemically (Zubo et al. 2018, Li et al. 2020). Results show that F_v/F_m and NPQ were similar in the respective tissues between MG and *alm1.g*-MG (**Supplementary Fig. S4**). Similar values in the two chlorophyll parameters suggest that, although their degrees of chloroplast development differed, both MG and *alm1.g*-MG spikes contained chloroplasts that are photosynthetically indistinguishable.

To investigate the extent to which the *alm1* mutation influences photosynthetic capacity, we used a portable chamber (6400; Li-Cor Inc.) to measure the carbon assimilation rate (photosynthesis ability) and two photochemical parameters (quantum yield and NPQ) under different light intensities. Quantum yield is the energy transfer efficiency of PSII under the light (Baker et al. 2008). Measurement of fully expanded second leaves at the third leaf stage plants indicated that MG and *alm1.g*-MG showed similar levels of photosynthesis and NPQ at any photon flux density up to $2,000 \mu\text{mol m}^{-2} \text{s}^{-1}$ tested, without significant differences (**Fig. 7A, C**). Quantum yield showed significant differences between the two lines, in a range of low-light conditions ($50\text{--}400 \mu\text{mol m}^{-2} \text{s}^{-1}$), but was similar in moderate light conditions (**Fig. 7B**).

Similarly, spike photosynthesis at the heading stage was measured using the system described above, when equipped with a special chamber encasing the main body of the spike excluding most awns. As expected from the chlorophyll deficient spikelet hulls in *alm1.g*-MG, the rate of carbon assimilation (photosynthesis ability) in *alm1.g*-MG spikes was significantly lower than that in MG, showing a 34% reduction (**Fig. 8**). These results, together with PAM chlorophyll measurements, indicated that *alm1.g*-MG is impaired in chloroplast development of restricted spike tissues rather than being defective in particular photosynthetic components.

Discussion

In this study, positional cloning indicated the barley *GLK2* transcription factor gene as a strong candidate of the *ALM1* locus. The conclusion, that *ALM1* encodes HvGLK2, is validated by genetic evidence showing that all ten *alm1* mutant alleles harbored a lesion in functionally important domains or motifs of the *HvGLK2* gene. *GLK* transcription factor genes are well-studied in other plant species (Chen et al. 2016). As discussed below, it is unexpected that the *alm1* mutant in barley was caused by mutations of the *HvGLK2* gene. The well-described roles of *GLK* transcription factor genes are control of chloroplast development in green and non-green tissues (Waters et al. 2009, Nakamura et al. 2009, Kobayashi et al. 2012). *GLK* proteins directly bind to the promoters of downstream target genes and activates transcription of genes related to light harvesting and chlorophyll biosynthesis (Waters et al. 2009). They further identified a 6-bp motif, CCAATC, as a putative *GLK cis*-element by promoter analysis of chromatin immunoprecipitation targets in *Arabidopsis thaliana*. The roles of *GLK* genes extended to control of disease resistance (Savitch et al. 2007), senescence (Rauf et al. 2013) and stomatal movement (Nagatoshi et al. 2016).

Barley *alm1* phenotypes devoid of chlorophyll pigments manifest both in floral (hulls, caryopsis pericarp and rachises) and non-floral (nodes and basal leaf sheaths) tissues (**Fig. 2, 3; Supplementary Fig. S2**). The tissues exhibiting the *alm1* phenotype seem to show a regular pattern. In floral tissues, the spikelet hulls and the rachis exhibit albinism in common. The spikelet has a sessile attachment to the rachis at each spike node. In non-floral tissues, basal leaf sheaths and nodes share albinism. Each leaf attaches at its sheath base to the node around the culm circumference. Consequently, the barley *alm1* phenotypes tend to appear in developmentally connected tissues. Albinism both in the lemma and palea, but not in the glume of the *alm1* mutants, is explainable by the degree of developmental relatedness, as proposed in the barley phytomer model of the spikelet (Forster et al. 2007, Franckowiak et al. 2010).

The severe barley *alm1* phenotype is in sharp contrast to no or mild phenotype in orthologous *glk2* mutants of other plant species, including *Arabidopsis thaliana*, tomato,

pepper, rice, and maize. In dicotyledons, *glk2* mutants exhibited a mild phenotype. Pale green siliques were observed in the *Atglk2* mutant plants of *Arabidopsis thaliana* (Fitter et al. 2002). A notable phenotype of the *Atglk2.1* mutant is a significant decrease of chlorophyll content in roots; this finding indicates a possible role of AtGLK2 controlling chloroplast development in roots (Kobayashi et al. 2012). Pale green fruits were found in a *Slglk2/uniform ripening* tomato mutant (Powell et al. 2012) and *Caglk2* pepper mutants (Brand et al. 2014). In monocotyledons, rice *Osglk2* mutant lines induced by a T-DNA insertion showed no visible phenotype (Wang et al. 2013). The original maize *g2* (syn. *Zmg2*) mutant had pale green leaf blades and whitish leaf sheaths (Jenkins, 1927, Neuffer et al. 1997), but two other allelic *g2* mutant lines caused by an *Spm* transposon insertion showed weak pale green leaf blades (Hall et al. 1998). Maize *g2* mutants gradually recovered their normal green color in leaf blades as they grew (Cribb et al. 2001).

Results obtained using TEM showed that the barley *alm1/Hvglk2* mutant had underdeveloped chloroplasts lacking thylakoid membranes and grana stacks in lemmas 6 days after heading (**Fig. 6**). The *glk2* single mutants of *Arabidopsis thaliana*, tomato, pepper and rice maintained thylakoid membranes and stacked grana in fruit or leaf chloroplasts without size changes (Fitter et al. 2002, Powell et al. 2012, Wang et al. 2013, Brand et al. 2014). Although the *glk1 glk2* double mutant plants of *Arabidopsis thaliana* and rice were entirely pale green throughout development, their leaf chloroplasts were diminished almost by half, while retaining rudimentary thylakoid membrane structures (Fitter et al. 2002, Wang et al. 2013). Consequently, the chloroplast phenotype was much more severe in barley *alm1/Hvglk2* lemmas than in leaves of the *Atglk1 Atglk2* and *Osglk1 Osglk2* double mutants (Fitter et al. 2002, Wang et al. 2013). Heavily underdeveloped chloroplasts in *alm1.g*-MG lemmas resembled those reported in albino leaf sectors of barley *CCT Motif Family gene 7 (cmf7)* mutant (syn. *albostrians*) (Li et al. 2019).

The *alm1* mutant allowed us to estimate photosynthesis ability in the main body of the barley spikes, excluding awns. Although leaf photosynthesis at the seedling stage was similar in MG and *alm1.g*-MG (**Fig. 7**), the *alm1.g*-MG spikes at the heading stage photosynthesized at the 66% rate of MG (WT) (**Fig. 8**). The 34% reduction in photosynthesis of the *alm1.g*-MG spikes parallels the 15.8% reduction in the 100-grain weight of the *alm1.g*-MG mutant plants (**Table 1**). However, one must consider the possibility that contributions of other green tissues can partly compensate for reduction of *alm1.g*-MG spike supplies. It is noteworthy that the chlorophyll content of flag leaves 5 days after heading was higher in *alm1.g*-MG than in MG (**Supplementary Table S4**). Additionally, cereals have the process of refixing CO₂ respired by the embryos and endosperm through seed-enclosing green tissues such as the pericarp layers, the lemma, and palea. Refixation of respired CO₂ is apparently a supplementary mechanism that is used to achieve more efficient spike photosynthesis (Tambissi et al. 2007). The refixation process is probably less effective in the *alm1.g*-MG spikes devoid of chlorophyll pigments. Taken together, although confounding of assimilates in spikes and

other parts precludes precise assessment of net spike assimilation, the present grain weight measurement in plural *alm1* mutants show the important photosynthetic role of green hulls in grain filling of barley (**Table 1; Supplementary Table S3**). The present results in barley would provide insight into spike photosynthesis research in wheat (*Triticum aestivum*) (Sanchez-Bragado et al. 2020, Simkin et al. 2020).

Detailed analyses of the *alm1* mutants of barley might present some implications for yield enhancement by manipulation of the *HvGLK2* gene. Barley breeding targeting the *HvGLK2* gene for efficient spike photosynthesis is apparently worth testing. Screening of barley genetic resources might identify natural variants with an elevated *HvGLK2* expression level. Alternatively, variants might be obtained by screening accessions with high chlorophyll accumulation in hulls. We have not yet attempted transgenic approaches to overexpress *HvGLK2* because *Agrobacterium*-mediated transformation is nearly impossible in predominant barley accessions (Hisano and Sato, 2016). In *Arabidopsis thaliana*, the *Atglk1 Atglk2* double mutants with an introduced *AtGLK1* gene driven by the silique-wall specific promoter were generated to test the silique-specific complementation line performance. These transgenic lines, restoring normal green siliques but retaining pale green leaves, had higher seed yield than *Atglk1 Atglk2* double mutant plants (Zhu et al. 2018). These results demonstrated that, in *Arabidopsis thaliana*, photosynthesis in silique wall is crucially important for seed yield.

The *alm1.g*-MG (*alm1.g*) mutant showed delayed heading by an average of 3.7 days compared with wild type. Heading delay of 2 to 4 days was reported for an *alm1.a* Bowman near isogenic line (Franckowiak and Lundqvist, 2016). These observations demonstrate that the *Hvglk2 (alm1)* mutant genes pleiotropically delay heading in barley. Waters *et al.* (2008) reported that, in *Arabidopsis thaliana*, *35S:AtGLK2* overexpression lines in the *Atglk1 Atglk2* double mutant background caused extreme delay of flowering compared with the wild type and the double mutant. Delayed flowering was evident under a long day condition. This observation implies that abundant GLK2 proteins suppressed flowering. In tomato, an *SIGLK2* signaling network model was proposed (Lupi et al. 2019). In this model, photoreceptor phytochromes first act as positive regulators of auxins (Bianchetti et al. 2017), which subsequently repress *SIGLK2* expression either directly or indirectly through an auxin response factor (ARF), *SIAFR4*, a negative regulator of auxin signaling (Sagar et al. 2013). The *SIGLK2* act as a master transcription factor to stimulate the differentiation of proplastids into chloroplasts (Chen et al. 2016). This model is unlikely to fit barley because the canonical ARF binding site, the TGTCTC, present in the *SIGLK2* gene, is not found within the 4 kb upstream promoter region of the barley *HvGLK2* gene sequence deposited in the Ensemble Plant database. Instead, the promoter of the *HvGLK1* gene had one ARF binding site in the 1,226-bp upstream region. In *Arabidopsis thaliana*, *AtGLK1* and *AtGLK2* reportedly interact with the NAC protein ORESARA 1 (ORE1), a key leaf senescence-control transcription factor. One report also suggests that ORE1 degrades the quality of chloroplasts through

antagonizing *AtGLK* transcription (Rauf et al. 2013). The barley *alm1/Hvglk2* mutants could be good materials to test this hypothesis.

In barley, no mutant of the paralogous *HvGLK1* gene (HORVU7Hr1G083690) has been identified to date. Our search of *Hvglk1* mutants failed because sequencing of this locus in six chlorophyll mutants mapped on chromosome 7H (four chlorina: *fch4.g*, *fch8.j*, *fch12.b*, *fch5.f*; two xantha: *xnt4.d* and *xnt9.i*; Lundqvist et al. 1997) did not detect any difference from their WT. Consequently, *HvGLK1* function can be inferred based solely on gene expression patterns and not on mutant phenotype. In both MG and *alm1.g*-MG lines, *HvGLK2* expression levels were rather high in leaves, moderate in awns and low in hulls. However, in both lines, *HvGLK1* expression was extremely weak in hulls compared to moderate levels in flag leaves and awns (**Fig. 5**). Such a differential expression pattern might explain a link of *HvGLK2* mutations with severe chlorophyll-less phenotypes manifested in hulls. Expression of the *HvGLK2* and *HvGLK1* genes in other tissues must be examined more precisely to complete the picture of where these two genes reduce or eliminate chloroplast development. Moreover, transcript levels of potential *HvGLK2* target genes, such as genes related to light harvesting and chlorophyll biosynthesis that were identified in *Arabidopsis thaliana* (Waters et al. 2009), need to be investigated in future study. In tomato, *SIGLK2* was found to be highly expressed in fruit (Powell et al. 2012, Nguyen et al. 2014); *SIGLK1* was predominantly expressed in leaves (Nguyen et al. 2014). Mutant and transgenic analyses revealed that differential expression patterns in tomato render (i) *SIGLK2* inhibition to pale green fruits, and (ii) *SIGLK1* suppression to pale green leaves (Nguyen et al. 2014). Consequently, mutants of the *GLK* transcription factors are widely divergent in the types of tissues affected and the magnitude of chlorophyll reduction among plant species. In conclusion, the severe and distinct *alm1* phenotypes of barley indicate that *HvGLK2* has some roles that are non-redundant with *HvGLK1*. Further mutant and transgenic analyses incorporating hitherto unavailable *Hvglk1* mutants could elucidate a unique feature of the *GLK* transcription factor network in barley.

Materials and Methods

Plant materials

For genetic mapping, we used an F₂ population of the cross between two linkage tester lines: KL15 with *alm1.a* and KL17. Barley *alm1* mutants and their wild type used for sequencing the *HvGLK2* gene are presented in **Supplementary Table S2**. A near isogenic pair of Misato Golden (MG) and its *alm1.g* mutant (*alm1.g*-MG) were used for detailed analyses of morphology, gene expression, photosynthesis activity, and agronomic traits. Agronomic traits were measured from plants grown in 21-cm diameter pots in an unheated glasshouse for two seasons (season 1 and season 2). In the respective seasons, nine and seven plants per genotype

were examined. Additionally, in 2019 (season 3), MG was compared with an *alm1.g*-MG (BC₂) isogenic line that were obtained by backcrossing twice to MG (WT); 20 individuals per genotype were planted in two rows in a container of 60 cm in length, and 20 cm in both width and height, without replication. Sowing dates were 12 October, 2015 (season 1), 23 September, 2016 (season 2), and December 25, 2019 (season 3). The heading date of each plant was scored as the day when the spike tip (excluding awns) emerged from the flag leaf sheath. Three spikes per plant were measured for culm length, spike length, awn length, number of grains per spike, and 100-grain weight. Awns were measured for those extended on the fourth spikelet from the top of the spike. For leaf and spike photosynthesis studies, plants were grown in 6 cm square pots. In addition, the effects of another *alm1* allele (*alm1.a*) on 100-grain weight were tested. We used a near isogenic pair of Bowman and *alm1.a*-Bowman with 8 times of backcrosses. Plants grown in an unheated greenhouse were tested for three years. Student's *t*-test was used for statistical comparisons throughout the study. Excel software was used for statistical processing. Barley seeds used in this study will be available upon request.

Positional cloning of *alm1*

The genetic mapping population comprised 157 F₂ plants derived from a cross between two linkage tester lines: KL15 with *alm1.a* and KL17. For mapping, DNA was isolated according to Taketa *et al.* (2012). Public SSR (Vershney *et al.* 2007) and EST (Sato *et al.* 2009) markers were used for initial mapping. Genetic mapping was conducted according to Yuo *et al.* (2012). New DNA markers for fine mapping were developed as described by Taketa *et al.* (2011). **Supplementary Table S1** presents their primer information. Primer pairs used for sequencing the *HvGLK2* gene in the *alm1* mutants and their wild type are presented in **Supplementary Table S5**. The genomic sequence of the *HvGLK2* gene in the Ensembl Barley database had a gap of unknown size in intron 1. To fill this gap, we attempted PCR amplification by designing various PCR primers at different positions in combination with the available *Taq* polymerases. The gap was filled by direct sequencing of PCR product using a primer pair of HvGLK2-LP3 and HvGLK2-RP4 combined with KOD-Plus-Neo DNA polymerase (Toyobo Co. Ltd.).

Phylogenetic analysis

The deduced amino acid sequences of GLK2 and GLK1 of barley were compared with homologous sequences of five other species (*Arabidopsis thaliana*, rice, maize, tomato and pepper). The accession numbers of deduced amino acid sequences in other species are AtGLK1 (AAK20120.1), AtGLK2 (AAK20121.1), OsGLK1 (LOC_Os06g24070.1), OsGLK2 (LOC_Os01g13740.1), ZmGLK1 (NP_001105018.1), ZmG2 (AAK50391.1),

SIGLK1 (AFM44934.1), SIGLK2 (AFM44933.1), CaGLK1 (AFF60405.1), and CaGLK2 (AFF60406.1). Phylogenetic trees were generated using CLUSTALW sequence alignment of the complete proteins using the neighbor-joining method (Saitou and Nei, 1987) available in the MEGA4 software package (Tamura et al. 2007).

Expression analysis of *HvGLK* genes

Hulls, awns, and flag leaves at the heading stage of MG and *alm1.g*-MG were collected separately and were used for RNA extraction. The heading stage is the time at which the spike fully emerged from the flag leaf sheath. Experiments were done with three biological replications. Total RNA was extracted using RNeasy Plant Mini Kit (Qiagen Inc.). Also, qRT-PCR was performed as described in an earlier report (Yuo et al. 2012). Briefly, for qRT-PCR, a first strand cDNA was synthesized with ReverTra Ace @qPCR_RT_Master_Mix (Toyobo Co. Ltd.). Quantitative analysis was conducted (Thermal cycle dice TP800; TaKaRa) using SYBR Premix DimerEraser (TaKaRa) according to the manufacturer's instructions. The barley *GAPDH* gene was used as an internal control to normalize the expression level of the target gene. The qRT-PCR primers are presented in **Supplementary Table S5**. Putative *cis*-regulatory elements within the GLK promoter region were predicted according to PLACE (<http://www.dna.affrc.go.jp/PLACE/>; Higo et al. 1999).

Chloroplast observation by TEM

For TEM, lemmas on the spikes 6 days after heading were cut into 2 × 2 mm pieces. The samples were fixed in 2% (w/v) paraformaldehyde and 2% (v/v) glutaraldehyde in 0.05 M cacodylate buffer, pH 7.4 at 4°C overnight. After this fixation, samples were washed three times with 0.05 M cacodylate buffer for 30 min each. They were postfixed with 2% osmium tetroxide in 0.05 M cacodylate buffer at 4°C for 3 h. Then the samples were dehydrated in graded ethanol solutions (50%, 70%, 90%, 100%). The samples were infiltrated two times with propylene oxide (PO) for 30 min each time and were put into a 70 : 30 mixture of PO and resin (Quetol-651; Nisshin EM Corp.) for 1 h. Then with the tube cap open, PO was volatilized overnight. For embedding, the samples were transferred to fresh 100% resin. They were polymerized at 60°C for 48 h. The polymerized resins were ultra-thin sectioned at 80 nm with a diamond knife using an ultramicrotome (Ultracut UCT; Leica Microsystems). Sections were stained with 2% uranyl acetate. They were secondary-stained with lead stain solution (Sigma-Aldrich Corp.). Sections were observed using a transmission electron microscope (JEM-1400Plus; JEOL) with acceleration voltage of 100 kV. Microscopic observations were made at Tokai Electron Microscopy.

Chlorophyll content and chlorophyll fluorescence measurements

The pair of MG (WT) and *alm1.g*-MG (mutant) near isogenic lines were planted in containers and were grown in a glasshouse. Detached spikes were studied at 5 or 16 days after heading. Chlorophyll contents were measured using a chlorophyll meter (SPAD-502Plus¹ Konica Minolta Holdings Inc.). The 16-day old spike samples were also analyzed using a two-dimensional chlorophyll fluorescence detection system (FluorCam800MF; Photon Systems Instruments) according to Kamau *et al.* (2015). Values for F_v/F_m and NPQ were obtained after dark adaptation of the organs for at least 15 min. Measurements were done with three replications in *alm1.g*-MG and MG near isogenic pair. Before separate measurement, spikes with a flag leaf were dissected into organs of four types: spikelets with awns, lateral spikelets, lateral spikelets on rachis, and spike rachis.

Photosynthesis activity in leaves and spikes

The pairs of MG (WT) and *alm1.g*-MG (mutant) near isogenic lines were grown in small pots. Leaf photosynthesis was measured in fully expanded second leaf blades of seedlings at the third leaf stage using a portable photosynthesis system (LI-6400XT; Li-Cor Inc.) as described by Kamau *et al.* (2015) with some modifications. Three individuals were studied for MG and *alm1.g*-MG mutant. The leaf chamber temperature was maintained at 25°C. The CO₂ concentration was maintained at 400 $\mu\text{mol mol}^{-1}$. The relative humidity was maintained as 70% – 80%. Leaves were acclimated in the chamber for approximately 30 min before measurements. Leaf photosynthesis rates were measured at different light intensity levels between 0 and 2,000 $\mu\text{mol m}^{-2} \text{s}^{-1}$. The measured chlorophyll parameters included the quantum yield and NPQ. For these measurements, the saturated light intensity was set as 7,500 $\mu\text{mol m}^{-2} \text{s}^{-1}$.

For spike photosynthesis measurements, the same system was equipped with a conifer chamber adapter (6400-05; Li-Cor Inc.). The main body of the spike was encased in the chamber. Inclusion of the surrounding awns was minimized. Spikes at the heading stage were measured for five individuals per genotype. The light intensity was $167 \pm 7.1 \mu\text{mol m}^{-2} \text{s}^{-1}$. Spikes were acclimated in the chamber for at least 30 min before measurements.

Funding

The work was supported partly by the Japan Society for the Promotion of Science [Grant-in-Aid for Scientific Research (No. 16K07556 to S.T.)]; the Brewers Association of Japan [to S.T.]; the Oohara Foundation [to M.H.].

Disclosures

The authors have no conflict of interest to declare.

Acknowledgements

We are grateful to U. Lundqvist, H. Bockelman, A. Kleinhofs, N. Kawada and T. Yoshioka for seed supply; J. Franckowiak for comments; and H. Kondo, M. Shiraga, M. Ikeda, A. Doi, F. Katayama and N. Hirose for technical assistance.

References

- Baker, N.R. (2008) Chlorophyll fluorescence: a probe of photosynthesis in vivo. *Annu. Rev. Plant Biol.* 59: 89-113.
- Bianchetti, R.E., Cruz, A.B., Oliveira, B.S., Demarco, D., Purgatto, E., Eustáquio, L. et al. (2017) Phytochromobilin deficiency impairs sugar metabolism through the regulation of cytokinin and auxin signaling in tomato fruits. *Sci. Rep.* 7: 7822.
- Brand, A., Borovsky, Y., Hill, T., Rahman, K.A.A., Bellalou, A., Deynze, A.V. et al. (2014) *CaGLK2* regulates natural variation of chlorophyll content and fruit color in pepper fruit. *Theor. Appl. Genet.* 127: 2139-2148.
- Chen, M., Ji, M., Wen, B., Liu, L., Li, S., Chen, X. et al. (2016) GOLDEN 2-LIKE transcription factors of plants. *Front. Plant Sci.* 7: 1509.
- Costa, J.M., Corey, A., Hayes, P.M., Jobet, C., Kleinhofs, A., Kopisch-Obusch, A. et al. (2001) Molecular mapping of the Oregon Wolfe barleys: a phenotypically polymorphic doubled-haploid population. *Theor. Appl. Genet.* 103: 415-424.
- Cribb, L., Hall, L.N. and Langdale, J.A. (2001) Four mutant alleles elucidate the role of the G2 protein in the development of C₄ and C₃ photosynthesizing maize tissues. *Genetics* 159: 787-797.
- Druka, A., Franckowiak, J., Lundqvist, U., Bonar, N., Alexander, J., Houston, K. et al. (2011) Genetic dissection of barley morphology and development. *Plant Physiol.* 155: 617-627.
- Fitter, D.W., Martin, D.J., Copley, M.J., Scotland, R.W. and Langdale, J.A. (2002) *GLK* gene pairs regulate chloroplast development in diverse plant species. *Plant J.* 31: 713-727.
- Forster, B.P., Franckowiak, J.D., Lundqvist, U., Lyon, J., Pitkethly, I. and Thomas, W.T.B. (2007) The barley phytomer. *Ann. Bot.* 100: 725-733.

- Franckowiak, J.D., Forster, B.P., Lundqvist, U., Lyon, J., Pitkethly, I. and Thomas, W.T.B. (2010) Developmental mutants as a guide to the barley phytomer. In Proc. Tenth Internat. Barley Genet. Symp. (Ceccarelli, S. and Grandi, S. eds). Alexandria Egypt: ICARDA, pp. 46-60.
- Franckowiak, J.D. and Lundqvist, U. (2016) Albino lemma 1. *Barley Genet. Newslett.* 46: 61-62.
- Gustafsson, A., Hagberg, A., Persson, G. and Wiklund, K. (1971) Induced mutations and barley improvement. *Theor. Appl. Genet.* 41: 239-248.
- Hall, L.N., Rossini, L., Cribb, L. and Langdale, J.A. (1998) GOLDEN 2: a novel transcriptional regulator of cellular differentiation in the maize leaf. *Plant Cell* 10: 925-936.
- Higo, K., Ugawa, Y., Iwamoto, M. and Korenaga, T. (1999) Plant *cis*-acting regulatory DNA elements (PLACE) database: 1999. *Nucleic Acids Res.* 27: 297-300.
- Hisano, H. and Sato, K. (2016) Genomic regions responsible for amenability to Agrobacterium-mediated transformation in barley. *Sci. Rep.* 6: 37505.
- Hua, W., Zhang, X-Q., Zhu, J., Shang, Y., Wang, J., Jia, Q. et al. (2016) Identification and fine mapping of a white husk gene in barley (*Hordeum vulgare* L.) *PLoS ONE* 11: e0152138.
- Imamura, A., Hanaki, N., Nakamura, A., Suzuki, T., Taniguchi, M., Kiba, T. et al. (1999) Compilation and characterization of *Arabidopsis thaliana* response regulators implicated in His-Asp phosphorelay signal transduction. *Plant Cell Physiol.* 40: 733-742.
- Jenkins, M.T. (1927) A second gene producing golden plant color in maize. *Am. Nat.* 60: 484-488.
- Kamau, P.K., Sano, S., Takami, T., Matsushima, R., Maekawa, M. and Sakamoto, W. (2015) A mutation in GIANT CHLOROPLAST encoding a PARC6 homolog affects spikelet fertility in rice. *Plant Cell Physiol.* 56: 977-991.
- Kobayashi, K., Baba, S., Obayashi, T., Sato, M., Toyooka, K., Keränen, M. et al. (2012) Regulation of root greening by light and auxin/cytokinin signaling in *Arabidopsis*. *Plant Cell* 24: 1081–1095.

Li, H., Ji, G., Wang, Y., Qian, Q., Xu, J., Sodmergen et al. (2018) WHITE PANICLE3, a novel nucleus-enclosed mitochondrial protein, is necessary for proper development and maintenance of chloroplasts and mitochondria in rice. *Front. Plant Sci.* 9: 762.

Li, M., Hensel, G., Mascher, M., Melzer, M., Budhagatapalli, N., Rutten, T. et al. (2019) Leaf variegation and impaired chloroplast development caused by a truncated CCT domain gene in *albostrians* barley. *Plant Cell* 31: 1430-1445.

Li, X., Wang, P., Li, J., Wei, S., Yan, Y., Yang, J. et al. (2020) Maize *GOLDEN2-LIKE* genes enhance biomass and grain yields in rice by improving photosynthesis and reducing photoinhibition. *Comm. Biol.* 3: 151.

Lundqvist, U., Franckowiak, J. and Konishi, T. (1997) New and revised description of barley genes. *Barley Genet. Newslett.* 26: 22-516.

Lundqvist, U. (2014) Scandinavian mutation research in barley – a historical review. *Hereditas* 151: 123-131.

Lupi, A.C.D., Lira, B.S., Gramegna, G., Trench, B., Alves, F.R.R., Demarco, D. et al. (2019) *Solanum lycopersicum* GOLDEN 2-LIKE 2 transcription factor affects fruit quality in a light- and auxin-dependent manner. *PLoS ONE* 14: e0212224.

Masher, M., Gundlach, H., Himmelbach, A., Beier, S., Twardziok, S.O., Wicker, T. et al. (2017) A chromosome conformation capture ordered sequence of the barley genome. *Nature* 544: 427-433

Milner, S.G., Jost, M., Taketa, S., Mazón, E.R., Himmelbach, A., Oppermann, M. et al. (2019) Genebank genomics highlights the diversity of a global barley collection. *Nat. Genet.* 51: 319-326.

Nagatoshi, Y., Mitsuda, N., Hayashi, M., Inoue, S., Okuma, E., Kubo, A. et al. (2016) GOLDEN 2-LIKE transcription factors for chloroplast development affect ozone tolerance through the regulation of stomatal movement. *Proc. Natl. Acad. Sci. USA* 113: 4218-4223.

Nakamura, H., Muramatsu, M., Hakata, M., Ueno, O., Nagamura, Y., Hirochika, H. et al. (2009) Ectopic overexpression of the transcription factor OsGLK1 induces chloroplast development in non-green rice cells. *Plant Cell Physiol.* 50: 1933-1949.

Neuffer, M.G., Coe, E.H. and Wessler, S.R. (1997) Mutants of maize. Cold Spring Harbor Library Press.

Nguyen, C.V., Vrebalov, J.T., Gapper, N.E., Zheng, Y., Zhong, S., Fei, Z. et al. (2014) Tomato *GOLDEN2-LIKE* transcription factors reveal molecular gradients that function during fruit development and ripening. *Plant Cell* 26: 585-601.

Nutbeam, A.R. and Duffus, C.M. (1978) Oxygen exchange in the pericarp green layer of immature cereal grains. *Plant Physiol.* 62: 360-362.

Powell, A.L.T., Nguyen, C.V., Hill, T., Cheng, K.L., Figueroa-Balderas, R., Aktas, H. et al. (2012) *Uniform ripening* encodes a *Golden 2-like* transcription factor regulating tomato fruit chloroplast development. *Science* 336: 1711-1715.

Rauf, M., Arif, M., Dortay, H., Matallana-Ramirez, L.P., Waters, M.T., Nam, H.G. et al. (2013) ORE1 balances leaf senescence against maintenance by antagonizing G2-like-mediated transcription. *EMBO Rep.* 14: 382-388.

Riechmann, J.L., Heard, J., Martin, G., Reuber, L., Jiang, C.-Z., Keddie, J. et al. (2000) *Arabidopsis* transcription factors: genome-wide comparative analysis among eukaryotes. *Science* 290: 2105-2110.

Rossini, L., Cribb, LC., Martin, D.J. and J.A. Langdale (2001) The maize *Golden2* gene defines a novel class of transcriptional regulators in plants. *Plant Cell* 13: 1231-1244.

Sagar, M., Chervin, C., Mila, I., Hao, Y., Roustan, J-P., Benichou, M. et al. (2013) SIARF4, an auxin response factor involved in the control of sugar metabolism during tomato fruit development. *Plant Physiol.* 161: 1362-1374.

Saitou, N. and Nei, M. (1987) The neighbor-joining method: A new method for reconstructing phylogenetic trees. *Mol. Biol. Evol.* 4: 406-425.

Sanchez-Bragado, R., Vicente, R., Molero, G., Serrot, M.D., Maydup, M.L. and Araus, J.L. (2020) New avenues for increasing yield and stability in C3 cereals: exploring ear photosynthesis. *Curr. Opin. Plant Biol.* 56: 223-234.

Sato, K., Nankaku, N. and Takeda, K. (2009) A high-density transcript linkage map of barley derived from a single population. *Heredity* 103:110-117.

Savitch, L.V., Subramaniam, R., Allard, G.C. and Singh, J. (2007) The GLK1 ‘regulon’ encodes disease defense related proteins and confers resistance to *Fusarium graminearum* in Arabidopsis. *Biochem. Biophys. Res. Commun.* 359: 234-238.

Shmakov, N.A., Gennadiy, V.V., Shatskaya, N.V., Doroshkov, A.V., Gordeeva, E.I., Afonnikov, D.A. et al. (2016) Identification of nuclear genes controlling chlorophyll synthesis in barley by RNA-seq. *BMC Plant Biol.* 16 (Suppl 3): 245.

Simkin, A.J., Faralli, M., Ramamoorthy, S. and Lawson, T. (2020) Photosynthesis in non-foliar tissues: implications for yield. *Plant J.* 101: 1001-1015.

Song, J., Wei, X., Shao, G., Sheng, Z., Chen, D., Liu, C. et al. (2014) The rice nuclear gene *WLPI* encoding a chloroplast ribosome L13 protein is needed for chloroplast development in rice grown under low temperature conditions. *Plant. Mol. Biol.* 84: 301-314.

Stadler, L.J. (1928) Mutations in barley induced by X-rays and radium. *Science* 68: 186-187.

Sun, J., Luu, N.S., Chen, Z., Chen, B., Cui, X., Wu, J. et al. (2019) Generation and characterization of a foxtail millet (*Setaria italica*) mutant library. *Front. Plant Sci.* 10: 369.

Takahashi, R. and Hayashi, J. (1959) Linkage study of albino lemma character in barley. *Ber. Ohara Inst. Landw. Biol., Okayama Univ.* 11: 132-140.

Taketa, S., Yuo, T., Sakurai, Y., Miyake, S. and Ichii, M. (2011) Molecular mapping of the short awn 2 (*lks2*) and dense spike 1 (*dsp1*) genes on barley chromosome 7H. *Breed. Sci.* 61: 80-85.

Taketa, S., Yuo, T., Tonooka, T., Tsumuraya, Y., Inagaki, Y., Haruyama, N. et al. (2012) Functional characterization of barley betaglucanless mutants demonstrates a unique role for CslF6 in (1,3;1,4)- β -D-glucan biosynthesis. *J. Exp. Bot.* 63: 381-392.

Tambussi, E.A., Bort, J., Guamet, J.J. Nogués, S. and Araus, J.L. (2007) The photosynthetic role of ears in C₃ cereals: Metabolism, water use efficiency and contribution to grain yield. *Crit. Rev. Plant Sci.* 26: 1-16.

Tamura, K., Dudley, J., Nei, M. and Kumar, S. (2007) MEGA4: Molecular Evolutionary Genetics Analysis (MEGA) software ver. 4.0. *Mol. Biol. Evol.* 24: 1596-1599.

- Varshney, R.K., Marcel, T.C., Ramsay, L., Russell, J., Röder, M.S., Stein, N. et al. (2007) A high density barley microsatellite consensus map with 775 SSR loci. *Theor. Appl. Genet.* 114: 1091-1103.
- Wang, P., Fouracre, J., Kelly, S., Karki, S., Gowik, U., Aubry, S. et al. (2013) Evolution of *GOLDEN2-LIKE* gene function in C₃ and C₄ plants. *Planta* 237: 481-495.
- Wang, Y., Wang, C., Zeng, M., Lyu, J., Xu, Y., Li, X. et al. (2016) WHITE PANICLE1, a Val-tRNA synthetase regulating chloroplast ribosomal biogenesis in rice, is essential for early chloroplast development. *Plant Physiol.* 170: 2110-2113.
- Waters, M.T., Moylan, E.C. and Langdale, J.A. (2008) GLK transcription factors regulate chloroplast development in a cell-autonomous manner. *Plant J.* 56: 432-444.
- Waters, M.T., Wang, P., Korkaric, M., Capper, R.G., Saunders, N.J. and Langdale, J.A. (2009) GLK transcription factors coordinate expression of the photosynthetic apparatus in *Arabidopsis*. *Plant Cell* 21: 1109-1128.
- Watson, P.A. and Duffus, C.M. (1988) Carbon dioxide fixation by detached cereal caryopses. *Plant Physiol.* 87: 504-509.
- Wykoff, D.D., Grossman, A.R., Weeks, D.P., Usuda, H. and Shimogawara, K. (1999) Psr1, a nuclear localized protein that regulates phosphorus metabolism in *Chlamydomonas*. *Proc. Natl. Acad. Sci. USA*, 96: 15336-15341.
- Yasumura, Y., Moylan, E.C. and Langdale, J.A. (2005) A conserved transcription factor mediates nuclear control of organelle biogenesis in anciently diverged land plants. *Plant Cell* 17: 1894-1907.
- Yoshikawa, T., Tanaka, S., Matsumoto, Y., Nobori, N., Ishii, H., Hibara, K. et al. (2016) Barley *NARROW LEAFED DWARF1* encoding a WUSCHEL-RELATED HOMEODOMAIN 3 (WOX3) regulates the marginal development of lateral organs. *Breed. Sci.* 66: 416-424.
- Yuo, T., Yamashita, Y., Kanamori, H., Matsumoto, T., Lundqvist, U., Sato, K. et al. (2012) A *SHORT INTERNODES* (*SHI*) family transcription factor gene regulates awn elongation and pistil morphology in barley. *J. Exp. Bot.* 63: 5223-5232.

Zubo, Y.O., Blakley, I.C., Franco-Zorrilla, J.M., Yamburenko, M.V., Solano, R., Kieber, J.J. et al. (2018) Coordination of chloroplast development through the action of the GNC and GLK transcription factor families. *Plant Physiol.* 178: 130-147.

Zhu, X.Z., Zhang, L., Kuang, C., Guo, Y., Huang, C., Deng, L. et al. (2018) Important photosynthetic contribution of silique wall to seed yield-related traits in *Arabidopsis thaliana*. *Photosyn. Res.* 137: 493-501.

Table 1. Agronomic characteristics of Misato Golden (MG) and *alm1.g*-MG isogenic lines in three independent trials

Season	Heading date	Culm length (cm)	Spike length (cm)	Awn length (cm)	No. grains per spike	100 grain weight (g)
2015/2016	(Date in April)					
	MG	13.4±1.6	60.5±2.9	5.8±0.4	7.5±0.3	24.4±0.8
	<i>alm1.g</i> -MG	17.2±1.2**	62.1±4.5	6.4±0.3 **	7.6±0.1	25.3±1.0
						(11.1%)
2016/2017	(Date in December)					
	MG	16.0±1.8	62.9±5.1	6.4±0.7	8.3±0.6	22.7±2.3
	<i>alm1.g</i> -MG	19.6±1.7**	66.1±4.5	6.7±0.5	8.7±0.6	21.7±2.6
						(22.2%)
2019/2020	(Date in March)					
	MG	23.0±1.4	67.5±3.4	6.3±0.3	6.4±0.2	29.0±1.6
	<i>alm1.g</i> -MG (BC ₂)	27.7±1.2**	72.5±3.4**	6.7±0.3**	6.4±0.3	29.4±1.4
						(14.1%)

Means and SD are shown. n=9 for 2015/2016, n=7 for 2016/2017 and n=20 for 2019/2020 season.

*, **: Significantly different at 5% and 1% levels, respectively. *t*-test was used.

(): Reduction rate (%) of 100 grain weight in *alm1.g*-MG mutant relative to WT control (MG).

Awn length was measured on the forth spikelets from the top of the spikes.

<Figure legends>

Fig. 1. Structure of the barley *ALBINO LEMMA 1* (*HvALMI*) gene in the cultivar Morex (standard), and nucleotide and amino acid changes found in ten *alm1* mutant lines. Blue boxes and yellow triangles respectively portray exons and introns with size (in bp) inside. The three alpha-helix domains are shown in magenta boxes. An AREAEAA motif in exon 3 is dark blue. The GCT box is shown in green. F.S. shows a frame shift resulting from a deletion.

Fig. 2. Barley *alm1* phenotypes in a near isogenic pair of Misato Golden (MG, WT) and *alm1.g* (*alm1.g*-MG) mutant. (A) Immature spikes. (B) Leaf blades. (C) Pericarp of immature caryopses. (D) Lemmas. (E) Paleae. (F) Culm nodes. (G) Basal leaf sheaths. Samples were about two-week-old spikes after heading. In all panels, the left is WT (MG). The right is *alm1.g* mutant. Bars are 1 cm in A and B, and 1 mm in C–G.

Fig. 3. Close-up images of immature spikes of two-rowed Misato Golden and six-rowed Morex barley with or without an *alm1* mutation. (A) Misato Golden (WT). (B) *alm1.g* mutant of Misato Golden. (C) Morex (WT). (D) *alm1.e* mutant of Morex. Spikes were about two weeks old after heading. In all figures, C and L (black) respectively portray central spikelet rows and lateral spikelet rows. Lowercase letters *g* (magenta) and *l* (blue) respectively show glumes and lemmas. Bars are 1 cm in A–D.

Fig. 4. Neighbor-joining phylogenetic tree of GLK2 and GLK1 proteins in six plant species. Numbers at the node signify bootstrap values of 1,000 trials.

Fig. 5. Quantitative RT-PCR analysis of expression of the *HvGLK2* (A) and *HvGLK1* (B) genes in three tissues (flag leaves, awns, and hulls) at the heading stage plants of Misato Golden (WT) and *alm1.g*-Misato Golden (*alm1.g* mutant). The *GAPDH* gene was used as an internal normalizer. Relative expressions of the *HvGLK2* and *HvGLK1* genes in respective tissues of WT and *alm1.g* are shown. Bars represent standard deviations of three biological replicates. Asterisks denote significant difference of *alm1.g* from WT in each tissue for respective gene: *, significant at the 5% level; **, significant at the 1% level; n.s., not significant.

Fig. 6. Transmission electron micrographs of chloroplasts in lemma cells 6 days after heading in Misato Golden (A and B) and *alm1.g*-MG (C and D). Bars are 1 μ m in (A) and (C); they are 5 μ m in (B) and (D). EM, envelope membranes; ST, non-stacked stroma thylakoid; GT, stacked grana thylakoid; V, vesicle.

Fig. 7. Photosynthetic capacity measured in fully expanded second leaves at the third leaf stage of Misato Golden (MG, WT) and *alm1.g*-MG. Photon flux density was 0 – 2,000 $\mu\text{mol m}^{-2} \text{s}^{-1}$: (A) photosynthesis ability (carbon assimilation rate). (B) Quantum yield. (C) Non-photochemical quenching (NPQ). Three plants were measured for each genotype. Bars are standard deviations. Significant differences between WT and *alm1.g* were marked by * (5% level) and ** (1% level). *t*-test was used.

Fig. 8. Photosynthesis ability of the spikes of Misato Golden (MG) and *alm1.g*-MG at the heading stage. Five plants were measured for each genotype. Bars represent standard deviations. ****, significant at the 0.01% level; *n*=5.

Supplementary data

Supplementary data are available at the PCP online.

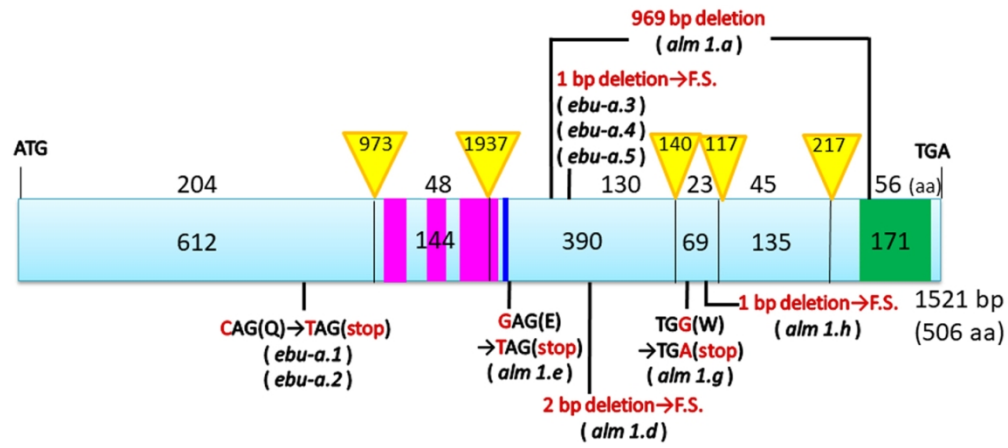


Fig. 1. Structure of the barley ALBINO LEMMA 1 (HvALM1) gene in the cultivar Morex (standard), and nucleotide and amino acid changes found in ten *alm1* mutant lines. Blue boxes and yellow triangles respectively portray exons and introns with size (in bp) inside. The three alpha-helix domains are shown in magenta boxes. An AREAEAA motif in exon 3 is dark blue. The GCT box is shown in green. F.S. shows a frame shift resulting from a deletion.

119x52mm (300 x 300 DPI)

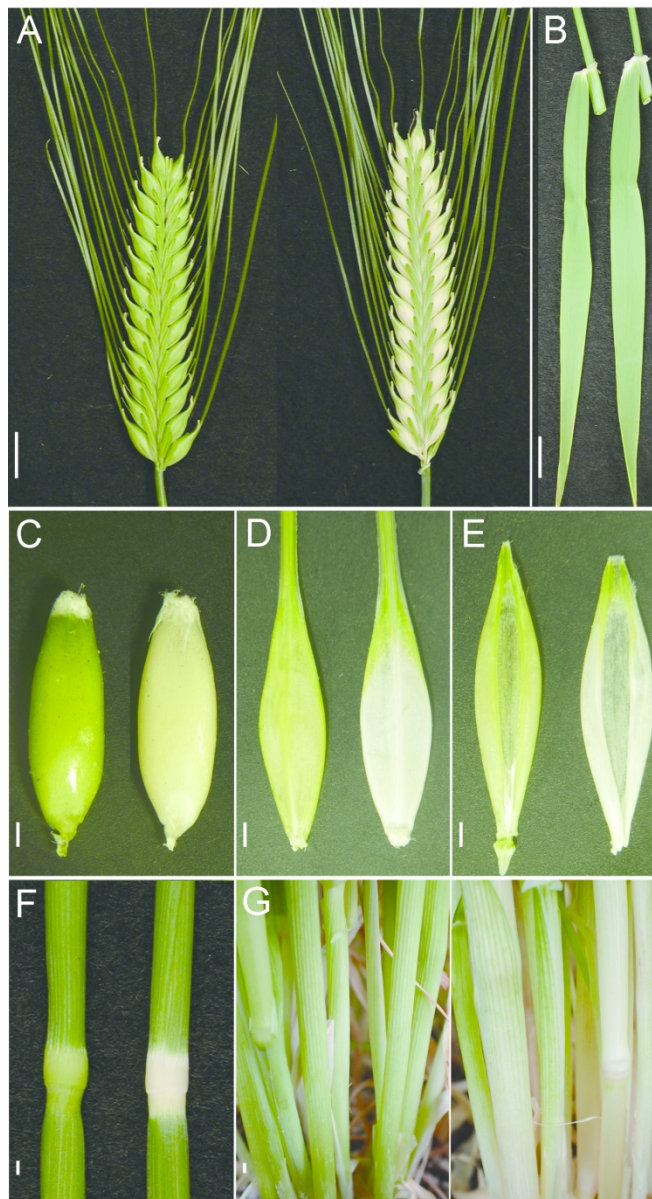


Fig. 2. Barley *alm1* phenotypes in a near isogenic pair of Misato Golden (MG, WT) and *alm1.g* (*alm1.g*-MG) mutant. (A) Immature spikes. (B) Leaf blades. (C) Pericarp of immature caryopses. (D) Lemmas. (E) Paleae. (F) Culm nodes. (G) Basal leaf sheaths. Samples were about two-week-old spikes after heading. In all panels, the left is WT (MG). The right is *alm1.g* mutant. Bars are 1 cm in A and B, and 1 mm in C–G.

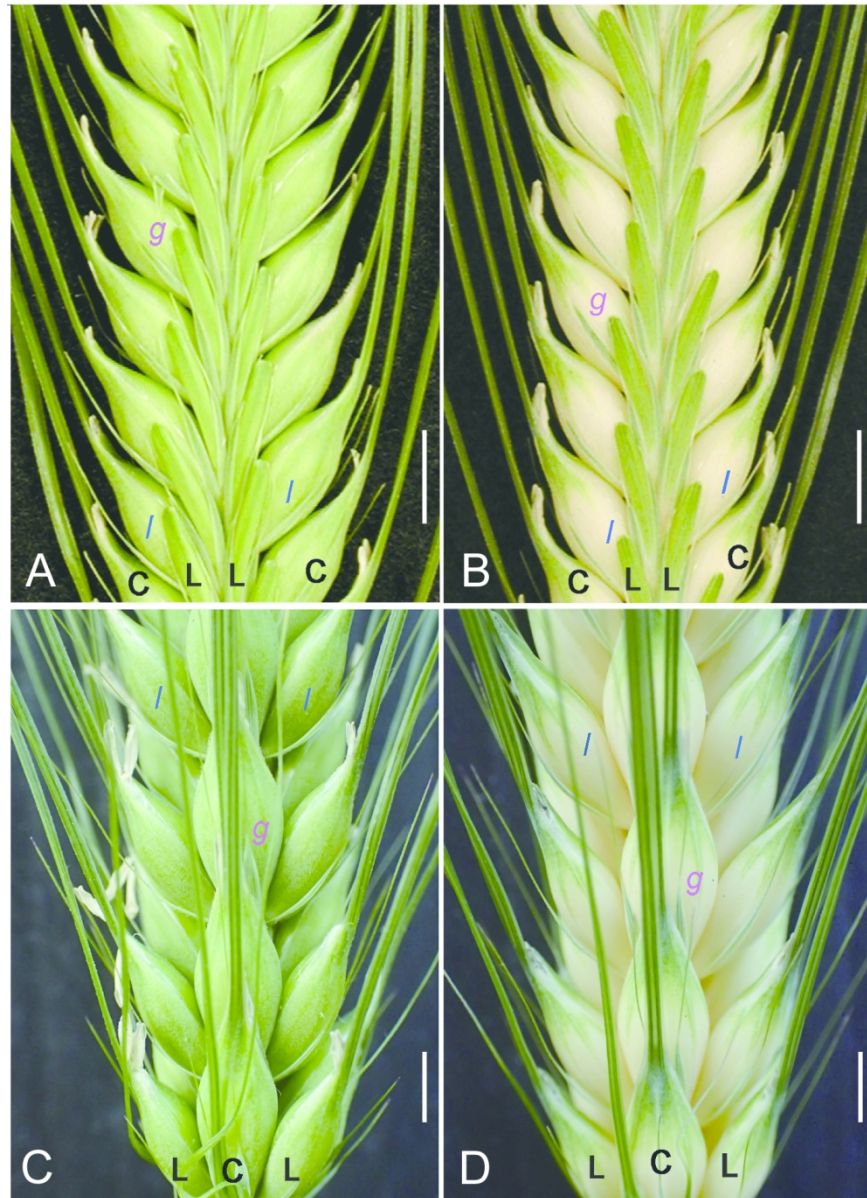


Fig. 3. Close-up images of immature spikes of two-rowed Misato Golden and six-rowed Morex barley with or without an *alm1* mutation. (A) Misato Golden (WT). (B) *alm1.g* mutant of Misato Golden. (C) Morex (WT). (D) *alm1.e* mutant of Morex. Spikes were about two weeks old after heading. In all figures, C and L (black) respectively portray central spikelet rows and lateral spikelet rows. Lowercase letters g (magenta) and l (blue) respectively show glumes and lemmas. Bars are 1 cm in A-D.

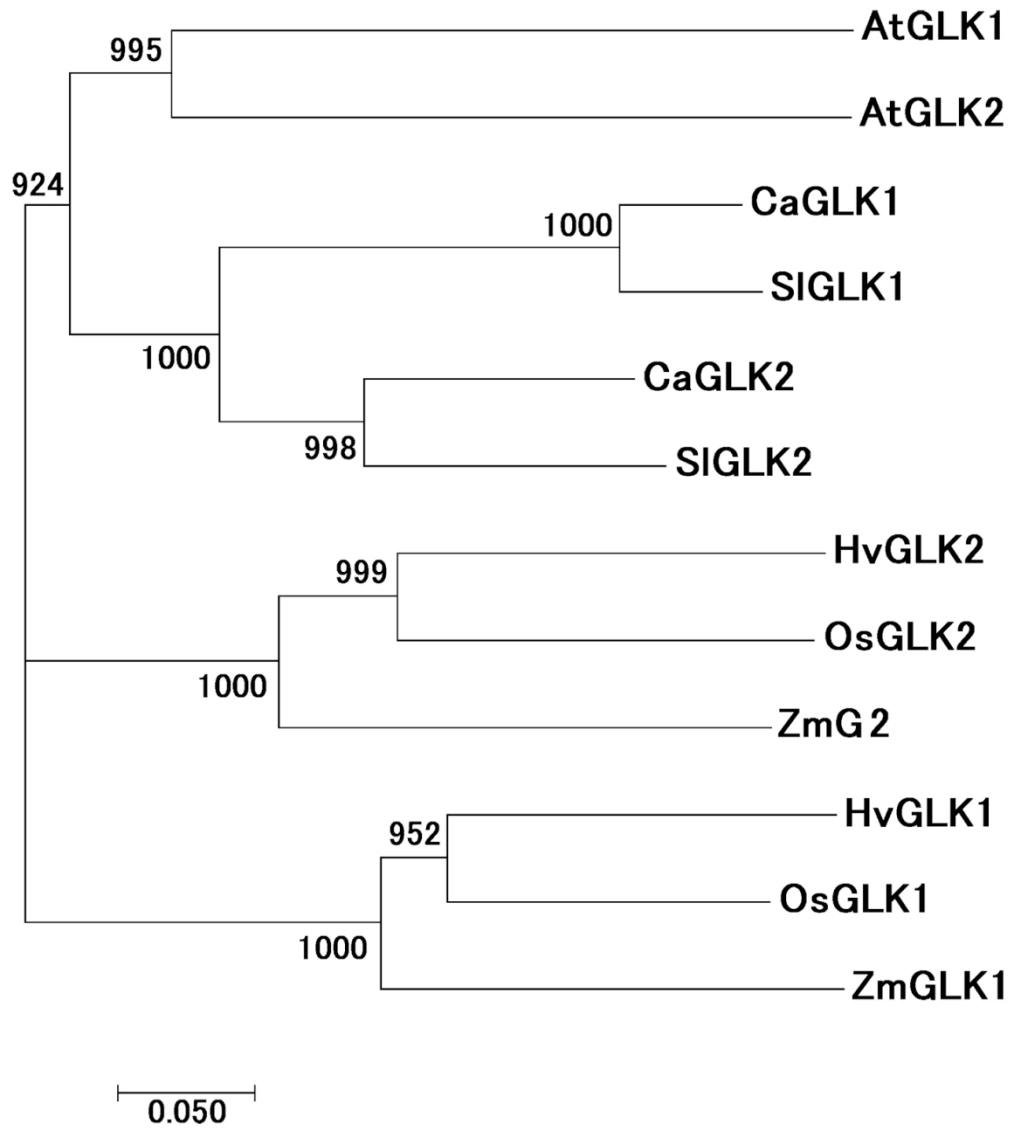


Fig. 4. Neighbor-joining phylogenetic tree of GLK2 and GLK1 proteins in six plant species. Numbers at the node signify bootstrap values of 1,000 trials.

119x135mm (300 x 300 DPI)

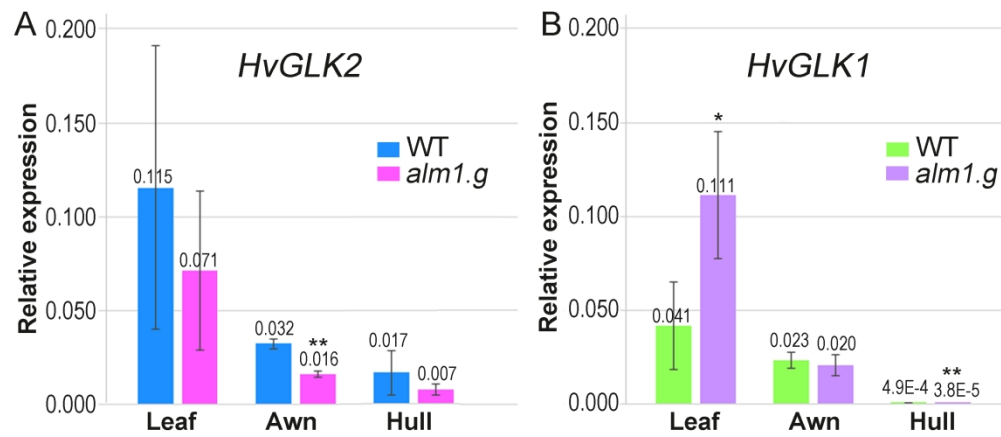


Fig. 5. Quantitative RT-PCR analysis of expression of the HvGLK2 (A) and HvGLK1 (B) genes in three tissues (flag leaves, awns, and hulls) at the heading stage plants of Misato Golden (WT) and alm1.g-Misato Golden (alm1.g mutant). The GAPDH gene was used as an internal normalizer. Relative expressions of the HvGLK2 and HvGLK1 genes in respective tissues of WT and alm1.g are shown. Bars represent standard deviations of three biological replicates. Asterisks denote significant difference of alm1.g from WT in each tissue for respective gene: *, significant at the 5% level; **, significant at the 1% level; n.s., not significant.

256x111mm (300 x 300 DPI)

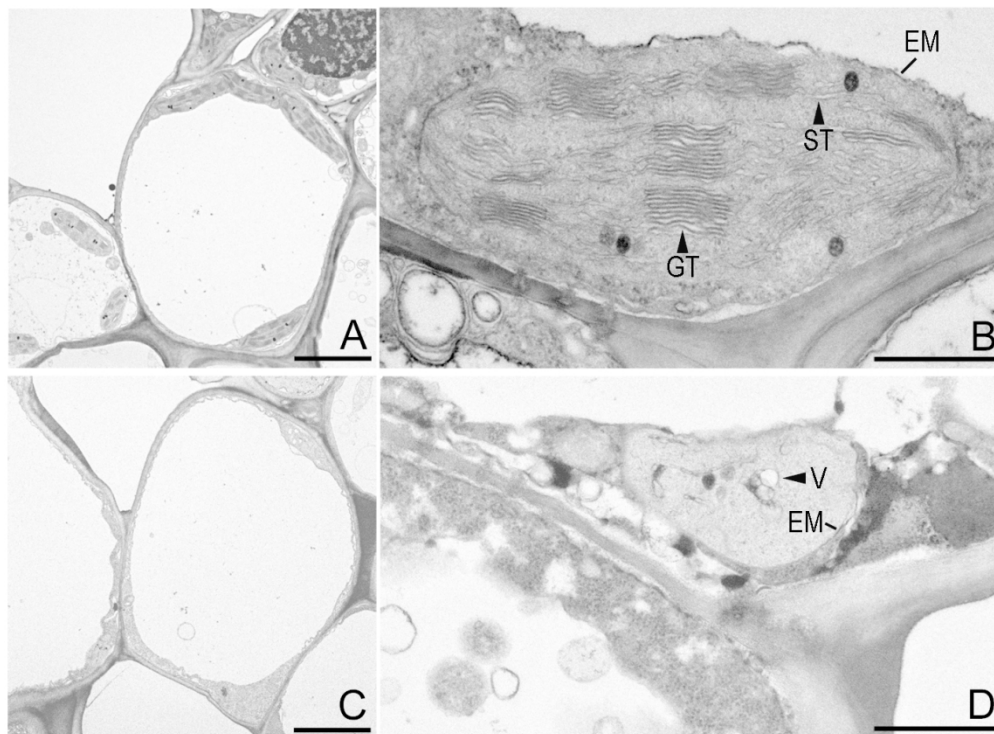


Fig. 6. Transmission electron micrographs of chloroplasts in lemma cells 6 days after heading in Misato Golden (A and B) and alm1.g-MG (C and D). Bars are 1 μm in (A) and (C); they are 5 μm in (B) and (D). EM, envelope membranes; ST, non-stacked stroma thylakoid; GT, stacked grana thylakoid; V, vesicle.

119x88mm (300 x 300 DPI)

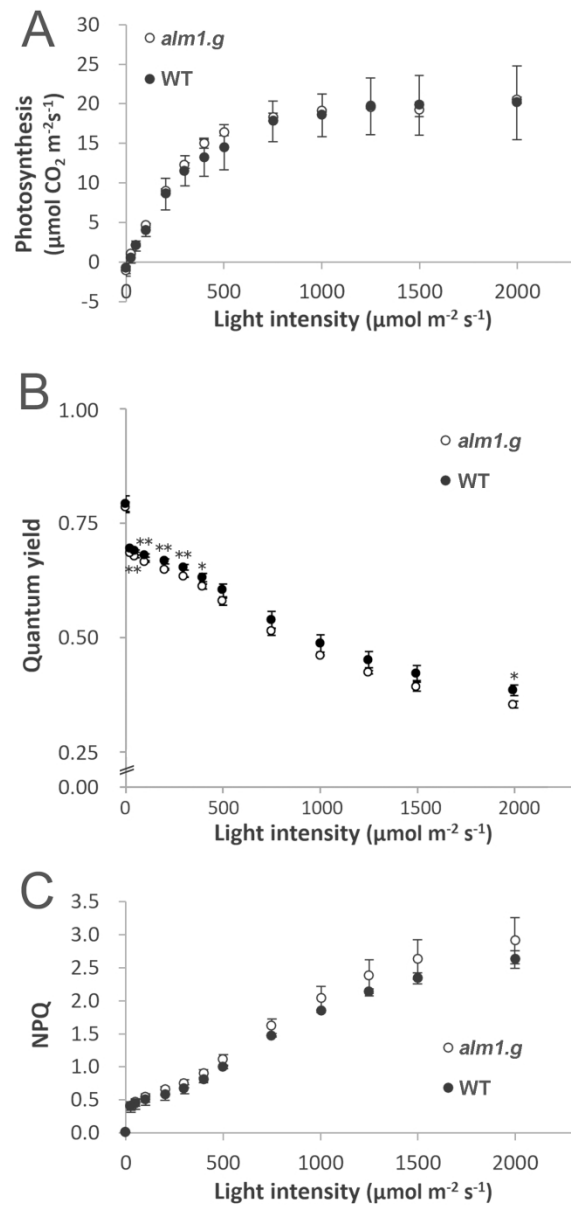


Fig. 7. Photosynthetic capacity measured in fully expanded second leaves at the third leaf stage of Misato Golden (MG, WT) and *alm1.g*-MG. Photon flux density was 0 – 2,000 $\mu\text{mol m}^{-2} \text{ s}^{-1}$: (A) photosynthesis ability (carbon assimilation rate). (B) Quantum yield. (C) Non-photochemical quenching (NPQ). Three plants were measured for each genotype. Bars are standard deviations. Significant differences between WT and *alm1.g* were marked by * (5% level) and ** (1% level). t-test was used.

119x251mm (300 x 300 DPI)

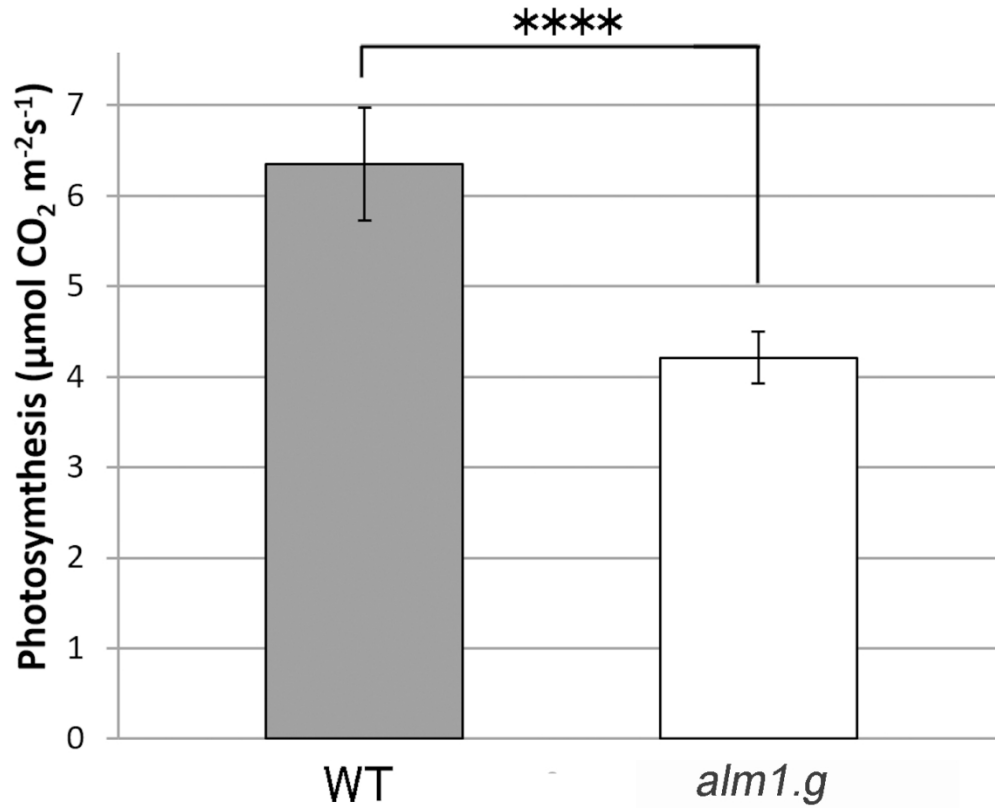


Fig. 8. Photosynthesis ability of the spikes of Misato Golden (MG) and *alm1.g*-MG at the heading stage. Five plants were measured for each genotype. Bars represent standard deviations. ****, significant at the 0.01% level; $n=5$.

119x97mm (300 x 300 DPI)

Supplementary Table S1. DNA markers for alm1 fine mapping that were originally developed for this study

Rice gene	Barley full length cDNA sequences for marker development	Barley marker name	Polymorphism detection	Primer (5'-3')	size (bp)*	Restriction enzyme	Fragment size after restriction enzyme digestion (bp)	Tm (°C)
LOC_Os01g13740	AK353571	HvGLK2	Length variation	LP9:ACTCGGAGTTAATGCGGTTG	708 (A)			55
	morex_contig_50813			RP11:CGTTTCTCACTTTTCGCAGA	1728 (B)			
LOC_Os01g13740	AK353571	HvGLK2-Indel	InDel	F1:GTCACACAGGAAGCACCTGA	523 (A)			55
	morex_contig_50813			R2d:GGCCATTACTGCAGCTAGTTC	674 (B)			
				R1:CCAGAGATCCATGTCAGTGC				
LOC_Os01g16530	AK364800	HvClp1	CAPS	LP3:AATGGCGAGAAATTGGGTTA	579 (A)	<i>Mbo I</i>	579 (A)	55
	morex_contig_48414			RP8:GGGGACAAGTTGGAGAAACA	584 (B)		231+353 (B)	
LOC_Os01g14440	AK35742	HvWRKY1	CAPS	LP4:GCATGAACGACGAGAACCAG	685 (A)	<i>Mse I</i>	685 (A)	55
	morex_contig_54547			RP4:TGCACGTACGGTAAGTCAGC	685 (B)		485+200 (B)	
LOC_Os01g17170	AK359877	HvCRD1	CAPS	LP4:CGAGGATCTTCCTGCTGTA	500 (A)	<i>Alu I</i>	53+183+264 (A)	55
	morex_contig_3412122			RP4:AAAAGTATCAACACAAGTTACATGACA	500 (B)		236+234 (B)	
					* (A): KL15, (B): KL17.			

Supplementary Table S2. Allelic variation of *alm1* mutants and their wild type in the HvGLK2 gene

Polymorphism		exon 1	intron 1	TTCCCG		CACCA		GCCG			intron 5							
				intron 2	exon 3	exon 4	exon 3	exon 4	intron 5									
nt position		418	703	3450	3709	3798	3818	3862	4211	4243	4666							
nt change		C → T	(G)n	C → T	G → T	Δ969	Δ1 C	Δ2 CA	G → A	Δ1 C	(AT)n					Caryopsis type		
aa change	Allele symbol	Q → *	—	—	E → *	—	P → R	H → S	W → *	P → R	—					c: covered, n: naked.	Row type	Seed source
aa position		140			267		303FS, 392*	318FS, 437*	387	398FS, 405*		Mutagen	Collection number					
Cultivar/ line		SNP1	SSR1	SNP2	SNP3	indel 1	indel 2	indel3	SNP4	indel4	SSR2							
Russia 82 <i>alm1.a</i>	<i>alm1.a</i>	C	20	C	G	969						spontaneous	GSH 270	c	6	USDA		
Bowman	WT	nt	nt	nt	nt	nt	nt	nt	nt	nt	nt	Original cultivar	PI 483239	c	2	USDA		
<i>alm1.a</i> -Bowman*8	<i>alm1.a</i>	nt	nt	nt	nt	nt	nt	nt	nt	nt	nt	Bowman near isogenic line for <i>alm1.a</i>	GSHO 1953	c	2	USDA		
Morex	WT	C	20	C	G	no	no	no	G	no	9	Original cultivar	Clho 15773	c	6	A. Kleinhofs		
Morex <i>alm1.d</i>	<i>alm1.d</i>	C	20	C	G	no	no	Δ2	G	no	9	gamma-rays	GSHO 3682	c	6	A. Kleinhofs		
Morex <i>alm1.e</i>	<i>alm1.e</i>	C	20	C	T	no	no	no	G	no	9	fast neutron	GSHO 3683	c	6	A. Kleinhofs		
Foma	WT	C	22	T	G	no	no	no	G	no	8	Original cultivar	NGB 14659	c	2	NordGen		
unknown <i>ebu-a.1</i>	<i>ebu-a.1</i>	T	22	T	G	no	no	no	G	no	8	ethylene imine	NGB 115236	c	2	NordGen		
Foma <i>ebu-a.2</i>	<i>ebu-a.2</i>	T	22	T	G	no	no	no	G	no	8	n-propyl methanesulfonate	NGB 115237	c	2	NordGen		
Foma <i>ebu-a.3</i>	<i>ebu-a.3</i>	C	22	T	G	no	Δ1	no	G	no	8	gamma-rays	NGB 115238	c	2	NordGen		
Foma <i>ebu-a.4</i>	<i>ebu-a.4</i>	C	21	T	G	no	Δ1	no	G	no	8	neutrons and ethyl methansulfonate	NGB 115239	c	2	NordGen		
Foma <i>ebu-a.5</i>	<i>ebu-a.5</i>	C	20	T	G	no	Δ1	no	G	no	8	ethyl methansulfonate	NGB 115240	c	2	NordGen		
Misato Golden	WT	C	20	C	G	no	no	no	G	no	8	Original cultivar	S 216	c	2	N. Kawada		
Misato Golden <i>alm1.g</i>	<i>alm1.g</i>	C	20	C	G	no	no	no	A	no	8	NaN ₃	S 249	c	2	N. Kawada		
Nanpu Hadaka	WT	C	21	C	G	no	no	no	G	no	8	Original cultivar	N-2 23	n	6	NARO Zentsuji		
Nanpu Hadaka <i>alm1.h</i>	<i>alm1.h</i>	C	21	C	G	no	no	no	G	Δ1	8	gamma-rays	N-1 205	n	6	NARO Zentsuji		

nt: not sequenced.

Supplementary Table S3. 100-grain weight of Bowman and its near isogenic <i>alm1.a</i> line with eight times of backcrosses				
Genotype	100-grain weight (g)			Average 100-grain weight (g)
	Season 1	Season 2	Season 3	of three seasons
Bowman (BW)	5.4	4.4	5.1	5.0±0.5
<i>alm1.a</i> -Bowman*8	4.0	3.9	3.5	3.8±0.3*
Reduction rate (%) of <i>alm1.a</i> -BW*8 relative to BW	(25.6)	(11.6)	(32.1)	(23.1)
Planting date	Jan. 13, 2013	Oct. 12, 2015	Nov. 22, 2016	
Harvest date	Jun. 27, 2013	Jun. 6, 2016	May 25, 2017	
A single plant per genotype was studied for each season. Five to 24 spikes per plant were bulked and measured for grain weight.				
*: Significantly different at the 5% level by t-test.				

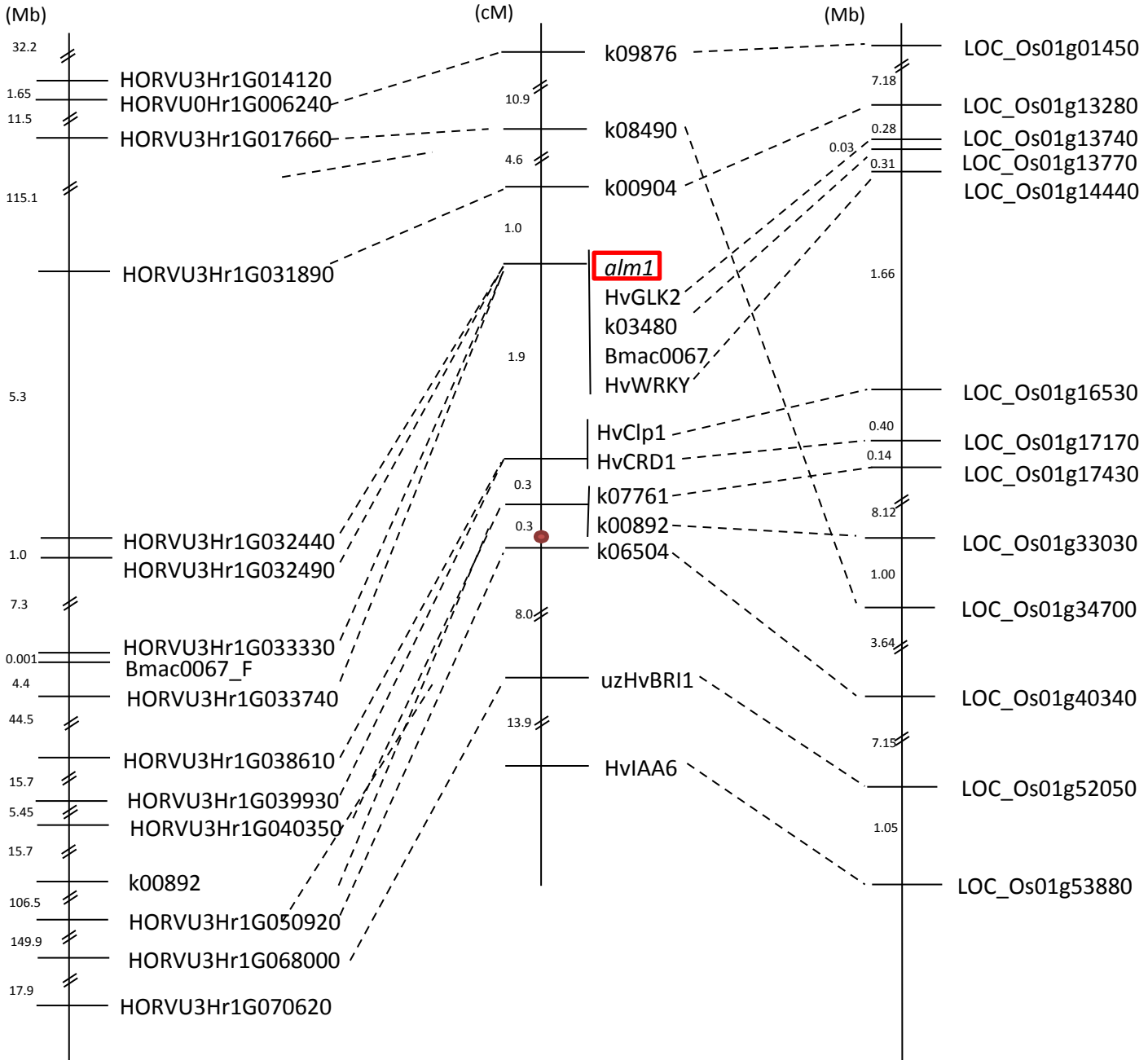
Supplementary Table S4. Changes of SPAD values in tissues of Misato Golden (MG, WT) and *alm1.g*-MG (*alm1.g* mutant)

Days after heading	Genotype	Lemma	Palea	Flag leaf
5 days	Misato Golden (MG)	5.2±0.8	1.5±0.2	45.2±1.0
	<i>alm1.g</i> -MG	n.d.	n.d.	49.9±0.6**
16 days	Misato Golden (MG)	10.6±2.4	4.1±2.3	n.t.
	<i>alm1.g</i> -MG	n.d.	n.d.	n.t.

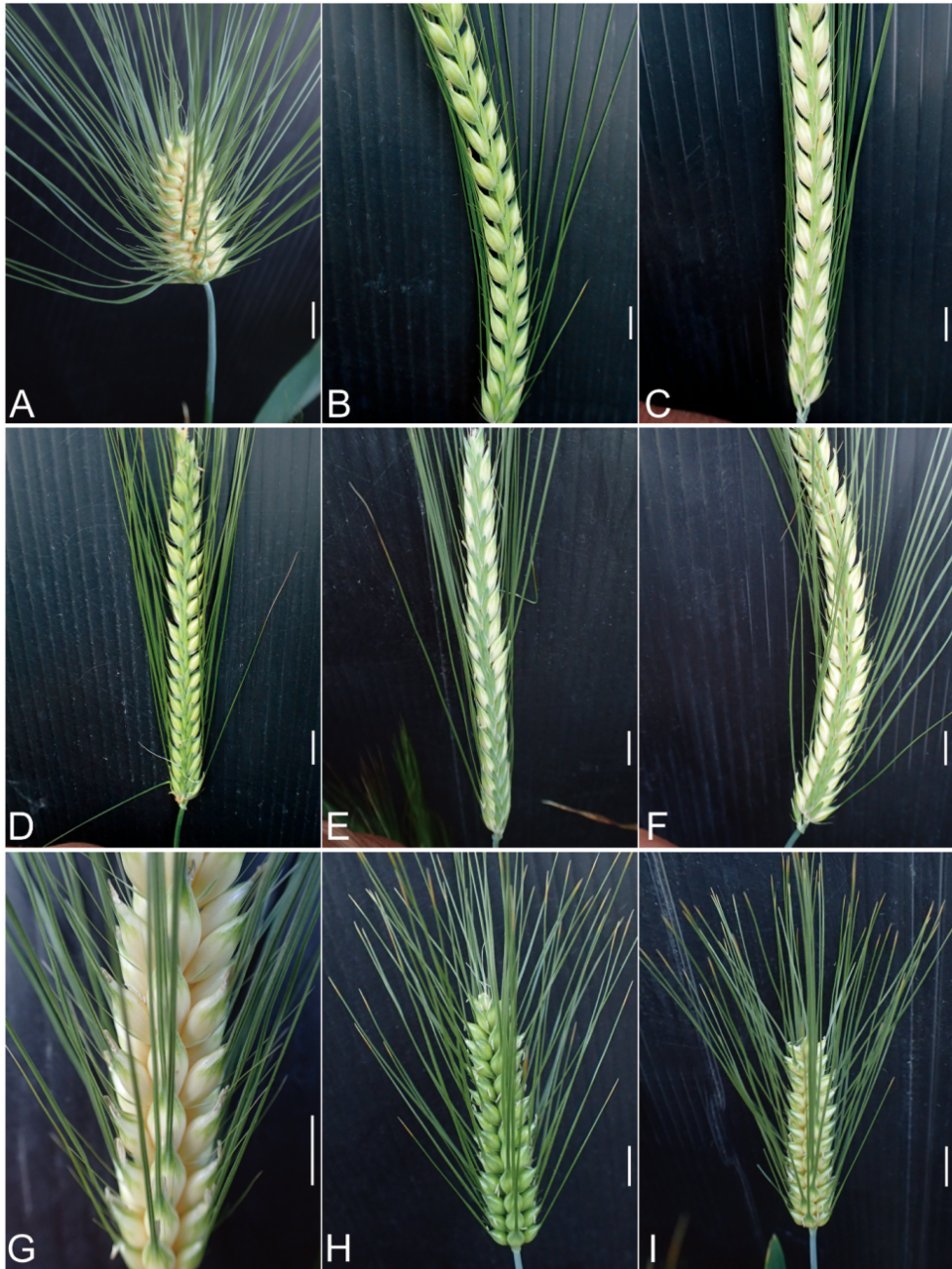
n.d.: below detection limit, n.t. : not tested , ** :p<0.01, n=3

Supplementary Table S5. Primers used for barley GLK2 genomic sequencing and qRT-PCR expression analysis

Forward Primer	5'→3'	Reverse Primer	5'→3'
HvGLK2-LP2	CAATTCGTTCCCATCTCTGC	HvGLK2-RP2	ATGCAGGGCAGTACCTTAC
HvGLK2-LP3	GTCCGAGAACAGCAAGTCGT	HvGLK2-RP3	GTCAGAGTTTACGCCAGACG
HvGLK2-LP3	GTCCGAGAACAGCAAGTCGT	HvGLK2-RP4	ACGCACGCACGTACGTATAG
HvGLK2-LP5	GGCGCCTATGAAAAGTCTTG	HvGLK2-RP5	CATGCTCGTGTTTGTCTTGG
HvGLK2-LP9	ACTCGGAGTTAATGCGGTTG	HvGLK2-RP11	CGTTTCTCACTTTTCGCAGA
HvGLK2-LP10	CTTTTGCTTTGCATGTTTGG	HvGLK2-RP10	TGCTCTCCTTGGACTGCATA
HvGLK2-LP13	CTAGCTCCACCTCCACGGTA	HvGLK2-RP13	GGGATTTCATGGCCTATTC
HvGLK2-LP15	ACATGGTCGTCATCAGTGGA	HvGLK2-RP15	ACCTGCGATTCCATCATTTTC
HvGLK2-LP16	TTCCACCATTTCATGCACATT	HvGLK2-RP16	TGGGTATACGTAGGCGAAGC
HvGLK2-LP17	ATCTGGCCATCTGGGTAACA	HvGLK2-RP17	AAAACGGGCGTAGTACATGG
HvGLK2-LP18	ATCGATCGTCGTTCCAGTTT	HvGLK2-RP18	GCCGGATAATTGCTTGAATC
HvGLK2-LP19	GCGGGGTGTTAAAAGTGAAA	HvGLK2-RP19	ACGGAGGGAGGGAGTACATT
HvGLK2-LP20	TGGCCATATCCTCACATGAA	HvGLK2-RP20	CCCAGACTACCAGGGATCAA
HvGLK2-LP21	CCCTCCGTTCCATAATGTTC	HvGLK2-RP21	TGCATGCGATGGTATAATGC
HvGLK2-LP22	CCCTACTCATGTGAGCCTGA	HvGLK2-RP22	TCAGGTGCTTCCTGTGTGAC
HvGLK2-LP23	GAGTTAATGCGGTTGCGTTT	HvGLK2-RP23	AGCCTGAGCGAGGAGAAAAT
HvGLK2-LP26	ATTTTCTCCTCGCTCAGGCT	HvGLK2-RP26	GCAACAGAAATCAGCAACCA
HvGLK2-LP27	GTGCCGAGAACAAATAAGGT	HvGLK2-RP27	CGAGTTGTGTCACCCAGAGA
HvGLK2-LP28	TGGTTGCTGATTCTGTTGC	HvGLK2-RP28	ATAGACGCAACAACCCTCGT
qRT-PCR primers	5'→3'		
GAPDH-F	GTGAGGCTGGTGCTGATTACG		
GAPDH-R	TGGTGCAGCTAGCATTGAGAC		
HvGLK2_AK353571-F5	ACTGGCACCAGCAGTACAAC		
HvGLK2_AK353571-R5	AGCAAACCTCTGCATCATGG		
HvGLK1_F2qRT-PCR	CCATGGGACTCCTTGAT		
HvGLK1_R2qRT-PCR	TAGCTGGAGCTGCGAATCTT		



Supplementary Fig. S1. Fine mapping of the *alm1* locus. The left is a physical map of barley chromosome 3H. The middle is a genetic map around the *alm1* locus. The red circle is the centromere. The right is a physical map of the syntenic region of rice chromosome.



Bar = 1 cm

Supplementary Fig. S2. Spike phenotypes of the remaining five *alm1* allelic mutants. (A) Russia 82 with the *alm1.a* allele. (B) wild type cv. Bowman. (C) Bowman near isogenic line with the *alm1.a* allele introduced by 8 times of backcrosses. (D) wild type cv. Foma. (E) Foma with the *ebu-a.2* allele. (F) Foma with the *ebu-a.3* allele. (G) Morex with the *alm1.d* allele. (H) wild type cv. Nanpu Hadaka. (I) Nanpu Hadaka with the *alm1.h* allele.

AtGLK1 1:MLALSPATRDGCD-----GASEFLDTSCGFTIINPEEEEEFPDFADHG-D 44
 AtGLK2 1:MLTVSPAP-VLIG-----NNSKDTYMAADFADFTTEDLPDFTTVGDFSD 44
 CaGLK1 1:MLAVS-PLSNTTA-----RDD--NTMESFGIGGG---VDFPDFVGEN-- 36
 SIGLK1 1:MLVVS-PFSNTTA-----RDERGNEMESFAIGGGGGGGDDFPDFMGEN-- 42
 CaGLK2 1:MLVSTPLSYKNE-----RGN-----YDLFQDFPDGN-- 27
 SIGLK2 1:MLALSSSLSYKNE-----REN-----YDLFQDFSHGN-- 27
 HvGLK2 1:MLEVATLQSPS---PAIFS---LGDHHVDVGFP-----EATVEDDDF 36
 OsGLK2 1:MLEVSTLRSPK---ADQRAG---VGGHHV-VGFVPAPPSPADVADEVD AFI VDDSC 49
 ZmG2 1:MLEVSTLRGPTSSGSKAEQHGGGGGGFVGDHVVFP TSG-----DCFAMVDDN 48
 HvGLK1 1:MLAVSSARCLAAD-----ADEQRAEAAPMETVGGAA-VVADLDIDFDF 42
 OsGLK1 1:MLAVSPAMCPDIE-----DRAAVAGDAGMEVVG---MSSDDMDQFDF 39
 ZmGLK1 1:MLAVSPSPVRCAD-----AEECGGGGASKEMEETAVGPVSDSDLDFDF 43

** ..

..

AtGLK1 45:LLDIIDFD--D--IFGVAG-D--VLPDLEIDPEIL-SGDFSNHMNASSTITTTSDKTD-- 94
 AtGLK2 45:LLDGIDYY--DDLFIGFDGDD--VLPDLEIDSEIL-G-EYSG--SGRDEEQEMEGNTS-- 94
 CaGLK1 37:LLDSIDFD--D-LFVGINDGD--VLPDLEMDTEIL-A-EFSVSSGDES DVNNYSSSNK-T 88
 SIGLK1 43:LLDSIDFD--D-LFVGINDGD--VLPDLEMDTEIL-A-EFSVSSGDES DVNNYSSSNNNN 95
 CaGLK2 28:LIDTIDFD--D-FFEGINDGD--LLQNLKI---L-D-EFDISK----- 60
 SIGLK2 28:LIDTINF D--D-FFDEINGGD--LLP-----DFEIFC----- 54
 HvGLK2 37:LLDYIDFSACDMPFFHVDDGDD I L P D L E V D P T E L - L A E F A D E P T T V L S P A P A P D G C E T H 95
 OsGLK2 50:LLEYIDFSCDVPFFHADDGD--ILPDLEVDPTEL-LAEFASSPDDEPPPTTSAPGPGE P 106
 ZmG2 49:LLDYIDFS-CDVPFFD-ADGD--ILPDLEVDTTEL-LAEFSSTPPADDLLAVAVFGADDQ 103
 HvGLK1 43:TVDDIDFG---DFFLRLEDGD--ALPDLEVDPADI-FTDLEAAAA--GVQELQDQVVP-C 93
 OsGLK1 40:SVDDIDFG---DFFLRLEDGD--VLPDLEVDPAEI-FTDFEAIATS-GGEGVQDQEVPTV 92
 ZmGLK1 44:TVDDIDFG---DFFLRLEDGD--ALPGLVDPAEIVFADF EAIATAGGDDGGVTDQEVPSV 99

... *.. . . . * *

AtGLK1 95:-----SQGETTKGSSGKGEVVSKR----- 114
 AtGLK2 95:-----TASERDVG---VCKQ----- 109
 CaGLK1 89:TFISTATKKVERKDETER---AASDVGSGLT-SLNQGEEIVSTQ----- 128
 SIGLK1 96:TFITTAIKNVERKEEIEKTGSVSASDVGSGLT TSLNQGEEIVSTQ----- 140
 CaGLK2 60:----- 60
 SIGLK2 54:----- 54
 HvGLK2 96:HHHG DDEKTTVETEPPEAEMMELPEGKGETKGLSSSSEEKDVKQQHDNDKNKKNNIVGD 155
 OsGLK2 107:AAAAGAKEDVKEDGAAAAAAAAAAYDGSPPPPRGKKKKDDEERSSSLPEEKDAKNGGGD 166
 ZmG2 104:PAAA-----VAQEKSSSLEQTCGDDKGVAVAAARRKLQTTTTTTTTTEEE----- 148
 HvGLK1 94:AFLAAVEDVGSVSSAGG-VGVEN-TAFGEEGRLGDEKRGCNQAEVG----- 138
 OsGLK1 93:ELLAPADDVGLDPCGDVVVGEEN-AAFAGAG---EEKGGCNQDD DAGE----- 137
 ZmGLK1 100:LPFADAAHIGAVDPCCG-VLGEDNDAACADVEEGKGEC DHADEVA AAGN----- 147



```

AtGLK1 115:-----DDVAAETVTYDGDSDRKRKYSSSASS-----KNNRISNNEGKRKVKVDWTPE 161
AtGLK2 110:-----EGGGGGDGGFRDKTVRRGKRKGKKS-----KDCLSDENDIKKKPKVDWTPE 155
CaGLK1 129:-----KSEESTLQVKQN-ITPKESDKGKKS-----KN----NLPVKRKVKVDWTPE 170
SIGLK1 141:-----KSEESTQQRNQNIIVTPKESDKGKKS-----KNH---NLPGKRKVKVDWTPE 184
CaGLK2 61:-----NNTTTNLNVK-TSKENDKSKKSS-----SQIK--NPEGKKKVKVDWTPE 102
SIGLK2 55:-----EPAIHGNMK-SKSKE---AKKSS-----SKIK--NPGGKKKVKLDWTPE 93
HvGLK2 156:EVCSAVTTDDSSAAVGSSENSKSSASAEGHSKR-----TSAAAATKSSHGRRKVKVDWTPE 210
OsGLK2 167:EVLSAVTTEDSSAGAAKS---CSPSAEGHSKRKPSSSSSSAAAGKNSHGKRKVKVDWTPE 223
ZmG2 149:-----DSSPAGSGAN--KSSASAEGHSSK-----KKSAGKNSNGGKRKVKVDWTPE 192
HvGLK1 139:-----ENMSGGDR---PIVPDAKSPSSTTSSSTEAESRHKSSGKSSHGKKAQVDWTPE 189
OsGLK1 138:-----ANVDDGAA---AVEAKSSSPSSTTSSSQEAESRHKSSSKSSHGKKAQVDWTPE 188
ZmGLK1 148:-----NNSDSGEAGCGGAFAGEKSPSSTASSSQEAESRRKVSCKHKSQGGKKAQVDWTPE 201

```

.. *. *. *****

Alpha-helix domain AREAEAA motif



```

AtGLK1 162:LHRRFVEAVEQLGVDKAVPSRILELMGVHC-LTRHNVASHLQKYRSHRKHLLAREAEAA 220
AtGLK2 156:LHRKFVQAVEQLGVDKAVPSRILEIMNVKS-LTRHNVASHLQKYRSHRKHLLAREAEAAS 214
CaGLK1 171:LHRRFVQAVEQLGVDKAVPSRILEIMGIDC-LTRHNIASHLQKYRSHRKHLLAREAEAAS 229
SIGLK1 185:LHRRFVQAVEQLGVDKAVPSRILEIMGIDC-LTRHNIASHLQKYRSHRKHLLAREVEEAAS 243
CaGLK2 103:LHRRFVKAIEKLGVDKAVPSRILELMATDG-LTRHNIASHLQKYRAHRKHLLAREAEAAS 161
SIGLK2 94:LHRKFVKAIEKLGVDKAVPSRILELMATHG-LTRHNIASHLQKYRAHRKHLLAREAEAAS 152
HvGLK2 211:LHRRFVQAVEQLGLDKAVPSRILELMGNEYRLTRHNIASHLQKYRSHRKHLMAREAEAAS 270
OsGLK2 224:LHRRFVQAVEQLGIDKAVPSRILELMGIEC-LTRHNIASHLQKYRSHRKHLMAREAEAAS 282
ZmG2 193:LHRRFVQAVEQLGIDKAVPSRILEIMGTDG-LTRHNIASHLQKYRSHRKHLMAREAEAAT 251
HvGLK1 190:LHRRFVQAVEQLGIDKAVPSRILEIMGINS-LTRHNIASHLQKYRSHRKHMMAREAEAAS 248
OsGLK1 189:LHRRFVQAVEQLGIDKAVPSRILEIMGIDS-LTRHNIASHLQKYRSHRKHMIAREAEAAS 247
ZmGLK1 202:LHRRFVQAVEELGIDKAVPSRILEIMGIDS-LTRHNIASHLQKYRSHRKHMLAREVEEAAT 260

```

. *. *. *. ** **. *. *****. *****. *****. ***. ***.

```

AtGLK1 221:WT-RKRHIY-----GVDTGANLNGRT--KNGWLAPAPTLGFPPPPP-----VA 260
AtGLK2 215:WN-LRRHAT-----VAVPGVGGGG---KKPWTAPA--LGYP-----H 246
CaGLK1 230:WS-QRRQLY-----CGAAVVGGGGKRDMPWPAP--TIGFPPPP----- 266
SIGLK1 244:WS-HRRQLY-----GGAPMVGGGGKREMNWPWPAP--TIGFPPPP-----LP 283
CaGLK2 162:WT-QRKQMY-----GGAIAIGGGGKRVIMNPWSAPP-TMGFP----- 196
SIGLK2 153:LN-HRKQMY-----SGATTIGGGGKRILMNPWPAPP-TMGFP----- 187
HvGLK2 271:WT-HKRQMY-----AAAGGPRKDAPAG---GGPWVVP--TVGFPPPGTMPHPHAAM 315
OsGLK2 283:WT-QKRQMYTAAAAAAVAAGGGPRKDAAAATAAVAPWVMP--TIGFPPP-----HAAAM 334
ZmG2 252:WA-QKRHMY-----APPAPRTTTTDD--AARPPWVPT--TIGFPPP----- 288
HvGLK1 249:WT-QRRQMY-----AAGGPAAAVKRQDSNMWTVP--TIGFAPP-----PPA 287
OsGLK1 248:WT-QRRQIY-----AAGG-GAVAKRPESNAWTVP--TIGFPPP-----PPP 284
ZmGLK1 261:WTTTHRRPMY-----AAPS--GAVKRPDSNAWTVP--TIGFPPP-----A 295

```

.. * * ..*..

AtGLK1 261: VAPPPVHHHFR-PLHVWGHPTVDQSIMPHVWPKHLPPPS----- 299
 AtGLK2 247: VAP--MHHGHFR-PLHVWGHPTWPKHKPNTPASAHRTYPM----- 283
 CaGLK1 267: -TMAAPMPHFR-PLHVWGHPSVDQSYMHWPKHLAPSPSPQHPSAWAPP--HLH---- 319
 SIGLK1 284: PPVAPPMPHFR-PLQVWGHPSVDQSYMHWPKHLAPSPSPQHPSAWAPPHHLH---- 338
 CaGLK2 197: -----PMAHHIR-PLHVWGHYPVNN----- 215
 SIGLK2 188: -----PMAHHVR-PLHVWGHYPVNN----- 206
 HvGLK2 316: AHHPGQPPFCR-PLHVWGHPTG----VDAPLPLSPPST--MLPVWRHLAPPP---- 364
 OsGLK2 335: VPPPPHPPFCRPLHVWGHPTAGVEPTTAAAPPPSPHAQPPLLPVWRHLAPPPPLP 394
 ZmG2 289: -----RFCR-PLHVWGHPPHAAAAEAAAATP-----MLPVWRHLAPPR--HL 329
 HvGLK1 288: PPPPAAMQHYAR-PLHVWGHPT----MDSRPMWMP-RHPMPRAPMPAWAP----- 332
 OsGLK1 285: PPSPAPIQHFR-PLHVWGHPT----MDPSRVPVWPPRHLVPRGPAPPWVP----- 330
 ZmGLK1 296: GTPRPVQHFGR-PLHVWGHPSPTAVESPRVPMWMP-RHLAPRAPPWWA----- 344

. * *. *****

AtGLK1 300: -----TAMPNPP-FWVSDSPYWHM-----HNGTTPYLPTVATRF 333
 AtGLK2 284: -----PAIAAPASWPGHPPYWH-----QQPLYP----- 307
 CaGLK1 320: -----PPPPSDPSFWHPHHQRVPNP-----LTPGTPYFPAPIAPT 354
 SIGLK1 339: -----PPPPLDPSFWHPHHQRVQNS-----LTPGTPYFPA--PT 370
 CaGLK2 216: -----SFWHPHYQGVVNS-----LAPGTPCFPSPT-- 240
 SIGLK2 207: -----SFWHPHYQRVNS-----LVPGTPCFPSAPITSA 234
 HvGLK2 365: -AWAH--QPPVDP-VYWHQQYNAARKWGPQAVT--QCVPPMPAAMMQRFAAPPMPG 416
 OsGLK2 395: AAWAHGHQAPVDPAAAYQQYNAARKWGPQAVTTPGTPCMPPLPPAAMLQRFVPPVPG 454
 ZmG2 330: APWAH--PTPVDP-AFWHQQYSAARKWGPQAAA-----VTQGTCPVPLPRFPVP---- 375
 HvGLK1 333: -----PPPPSDPAFWHHPYMRGPAAYMPTHG-----TPCMAMP-APKFPAPPVPV 378
 OsGLK1 331: -----PPPP-SDPAFWHHPYMRGP-AHVPTQG-----TPCMAMPMPAARFPAPPVPG 375
 ZmGLK1 345: -----PPPPADPASFWHHPYMRGPAAHMPDQVA-----VTPCVAVPMAAARFPAPHVRG 393

. . . *

GCT box

AtGLK1 334: RAPPVAGIPHALPPHHTMYKPNLGF-----GARPPVDLHPSKESVDAAG 379
 AtGLK2 308: -----QGYGMASNHSSIGVPTRQLG-----PTNPPIDIHPSNESIDAAIG 348
 CaGLK1 355: RYPGGHHPVPGIPP-AAHAMYKVDH----VRSTAP-PTQPLPKPCDFHPSKESIDAAIG 408
 SIGLK1 371: RYP-----VPGIPPSSHGMKYVDQSNIGVRSTATLPAQPLPEPPCDFHPSKESIDAAIG 425
 CaGLK2 241: RFAAPL-MVPGVPPP-----FASRQTP-----HLHPTKESIDAAIE 275
 SIGLK2 235: RFAAPL-MVPGIPPSPAIKVDTVAS-----DLHPSNESIDAAIE 273
 HvGLK2 417: MMPHPMY-RPIPPSPVPQNNKAVG-----LQLQLDAHPSKESIDAAIG 460
 OsGLK2 455: MVPHPMY-RPIPPSP--PQGNKLA-----LQLQLDAHPSKESIDAAIG 496
 ZmG2 376: ---HPIYSRPAMVPPP--PSTTKLAQ-----LHLELQAHPKESIDAAIG 415
 HvGLK1 379: AMPCP--VYAPPSPALASKSQDS-----QLQLSQSPNESIDAAIG 420
 OsGLK1 376: VVPCP--MYRPLTP-PALASKNQDA-----QLQLVQPSSESIDAAIG 416
 ZmGLK1 394: SLPWPPMYRPLVP-PALAGKSQDA-----LFQLQIQPSSESIDAAIG 436

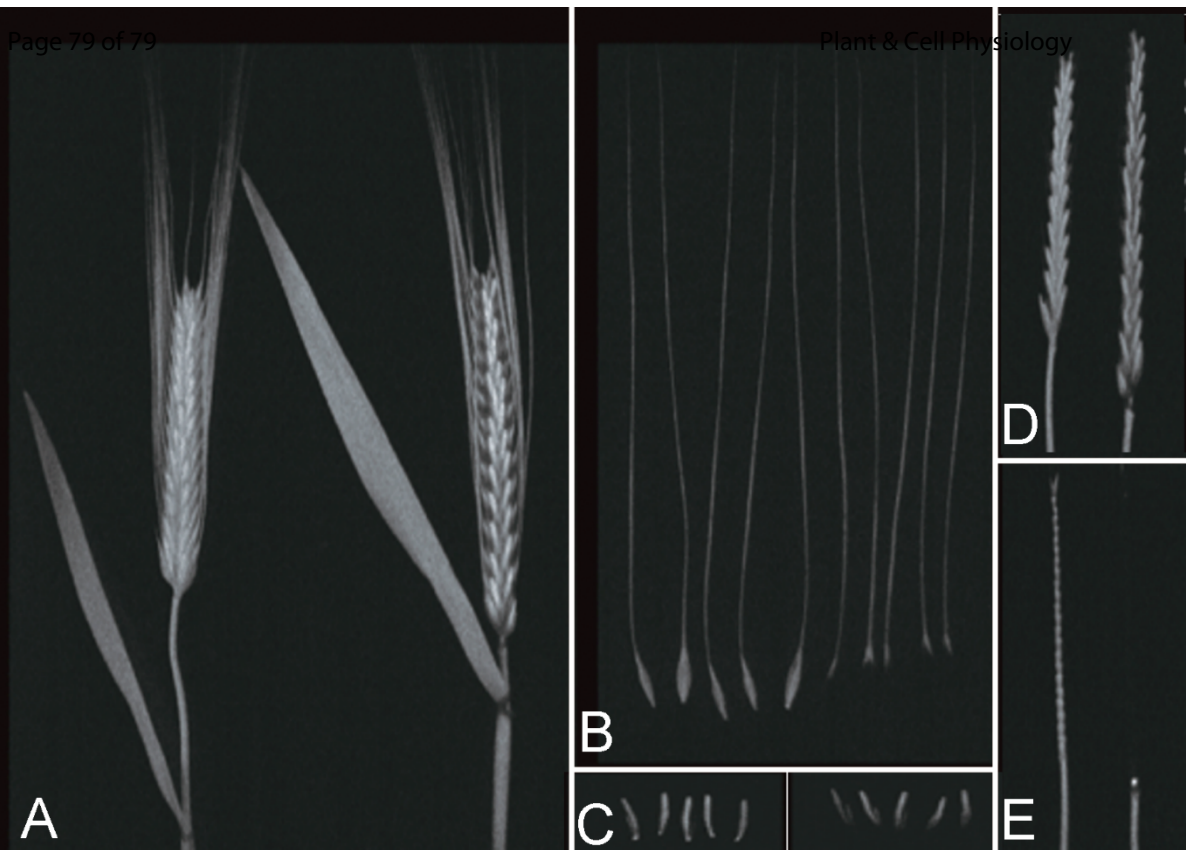
. . * . * . *****

GCT box

AtGLK1	380:DVLTRPWLPLPLGLNPPAVDGVMTLHRHGVSEVPPTASCA-----	420
AtGLK2	349:DVISKPWLPLPLGLKPPSVGDVMTLQRQGVSNVPLP-----	386
CaGLK1	409:DVLSKPWLPLPLGLKPPAVDSVLGELQRQGVPKIPPTCA-----	447
SlGLK1	426:DVLSKPWLPLPLGLKPPAVDSVLGELQRQGVPKIPPTCA-----	464
CaGLK2	276:DVLSKPQTLPPIGLKPPSIDSVLNELQCQGITKIPPT-----	312
SlGLK2	274:DVLSKPQLPLPIGLKPPSIDSVLNELQRQGITKIPPT-----	310
HvGLK2	461:DVLVKPWLPLPLGLKPPSLDSVMSELHKQGIPKVPPAATTNCDGAA-	506
OsGLK2	497:DVLVKPWLPLPLGLKPPSLDSVMSELHKQGIPKVPPAAS----GAAG	539
ZmGL2	416:DVLVKPWLPLPLGLKPPSLDSVMSELHKQGVKIPPAATT-TGATG	461
HvGLK1	421:DVLSKPWLPLPLGLKPPSLGSVMGELERQGVANVPQACG-----	459
OsGLK1	417:DVLSKPWLPLPLGLKPPSVDSVMGELQRQGVANVPPACG-----	455
ZmGLK1	437:DVLTKPWLPLPLGLKPPSVDSVMGELQRQGVANVPQACG-----	475

...*.*.**.**...*.**...*...*

Supplementary Fig. S3. Multiple alignment of deduced amino acid sequences of the *Golden2-like* transcription factor genes from *Arabidopsis thaliana* (At), *Capsicum annuus* (Ca), *Solanum lycopersicum* (Sl), *Hordeum vulgare* (Hv), *Oryza sativa* (Os), and *Zea mays* (Zm). Highly conserved amino acid residues in the alpha-helix domain (dark blue in three parts), an AREAEAA motif (orange) and the GCT-box (green) are marked with horizontal bars of different colors above the alignment. Exceptional V residues within an AREAEAA motif are highlighted in red. An AARKW motif conserved among the *GLK2* genes of barley, rice, and maize is highlighted in magenta.



Tissue	Genotype	Fv/Fm	NPQ
(A) Spike with a flag leaf	MG (WT)	0.84 ± 0.006	3.29 ± 0.200
	<i>alm1-MG</i>	0.84 ± 0.010	2.83 ± 0.127
(B) Spikelets with an awn	MG	0.84 ± 0.004	3.08 ± 0.171
	<i>alm1-MG</i>	0.83 ± 0.007	2.80 ± 0.096
(C) Lateral spikelets	MG	0.81 ± 0.019	3.40 ± 0.543
	<i>alm1-MG</i>	0.81 ± 0.012	2.65 ± 0.527
(D) Lateral spikelets on rachis	MG	0.84 ± 0.006	3.29 ± 0.200
	<i>alm1-MG</i>	0.84 ± 0.010	2.83 ± 0.127
(E) Spike rachis	MG	0.85 ± 0.010	2.78 ± 0.610
	<i>alm1-MG</i>	0.83 ± 0.017	2.41 ± 0.730

Supplementary Fig. S4. Chlorophyll fluorescence in the detached spikes with a flag leaf. Spikes at the stage of 16 days after heading were examined. In all panels, the left shows MG (WT); the right shows *alm1.g-MG* (*alm1.g* mutant). (A) Spikes with a flag leaf. (B) Spikelets with an awn. (C) Lateral spikelets. (D) Lateral spikelets on rachis. (E) Spike rachis. The bottom half shows two photosynthesis parameters, Fv/Fm and NPQ, of the respective panel images.